

Northumbria Research Link

Citation: Combrinck, Madeleine, Harms, Thoman, McGeoch, Melodie, Schoombie, Janine and Le Roux, Peter (2020) Wind and seed: a conceptual model of shape-formation in the cushion plant *Azorella Selago*. *Plant and Soil*, 455 (1-2). pp. 339-366. ISSN 0032-079X

Published by: Springer

URL: <https://doi.org/10.1007/s11104-020-04665-3> <<https://doi.org/10.1007/s11104-020-04665-3>>

This version was downloaded from Northumbria Research Link:
<http://nrl.northumbria.ac.uk/id/eprint/44073/>

Northumbria University has developed Northumbria Research Link (NRL) to enable users to access the University's research output. Copyright © and moral rights for items on NRL are retained by the individual author(s) and/or other copyright owners. Single copies of full items can be reproduced, displayed or performed, and given to third parties in any format or medium for personal research or study, educational, or not-for-profit purposes without prior permission or charge, provided the authors, title and full bibliographic details are given, as well as a hyperlink and/or URL to the original metadata page. The content must not be changed in any way. Full items must not be sold commercially in any format or medium without formal permission of the copyright holder. The full policy is available online: <http://nrl.northumbria.ac.uk/policies.html>

This document may differ from the final, published version of the research and has been made available online in accordance with publisher policies. To read and/or cite from the published version of the research, please visit the publisher's website (a subscription may be required.)



**Northumbria
University**
NEWCASTLE



UniversityLibrary

Wind and seed: a conceptual model of shape-formation in the cushion plant *Azorella Selago*

Madeleine L. Combrinck^{1,2*}, Thomas M. Harms¹, Melodie A. McGeoch³, Janine Schoombie⁴, Peter Christiaan le Roux^{4,5}

¹ Department of Mechanical and Mechatronic Engineering, Stellenbosch University, South Africa

² Department of Mechanical and Construction Engineering, University of Northumbria, United Kingdom

³ School of Biological Sciences, Monash University, Clayton 3800, Victoria, Australia

⁴ Department of Plant and Soil Sciences, University of Pretoria, South Africa

⁵ Center for Invasion Biology, Department of Botany and Zoology, Stellenbosch University, South Africa

* Author for correspondence: Madeleine Combrinck. Telephone: +44 (0) 191 227 4549. Email: madeleine.combrinck@northumbria.ac.uk

Abstract

Aims

Winds can strongly affect the growth, and therefore shape, of individual plants. The sub-Antarctic cushion plant, *Azorella selago*, is usually hemispherical when small but frequently crescent-shaped when larger. Here spatial variation in wind speed and in air-borne seed and sediment deposition is examined to determine if wind scouring and/or deposition patterns could contribute to the development of non-hemispherical shapes in cushion plants.

Methods

Computational fluid dynamic analyses were conducted for hemispherical and crescent-shaped cushion plants. Models were parameterized with data from *A. selago* and *A. magellanica* habitats on Marion Island. The numerical data were contextualized with field observations and sources in the literature to arrive at a conceptual model for shape development.

Results

Airflow modelling, supported by field data, showed that both wind scouring and seed deposition of the commonly co-occurring grass *Agrostis magellanica* are greater on the windward side of the cushion plant but seed are subjected to a high mortality rate in this region. By contrast, heavier sediment particles are predominantly deposited on the leeward side of plants, leading to the burial of lee-side *A. selago* stems. This sediment accumulation may initiate the development of the crescent-shape in hemispherical plants by increasing stem mortality on the plant's leeward edge. Once developed, the crescent-shape is probably self-reinforcing because it generates greater air recirculation (and lower air velocities) which enhances further seed and sediment deposition and establishment of *A. magellanica* grasses in the lee of the crescent. The conceptual model consists therefore of three stages namely, (1) negligible air recirculation, (2) sediment deposition and grass establishment, and (3) differential cushion growth.

Conclusion

This conceptual model of cushion plant shape development may explain the occurrence and orientation of crescent-shaped cushion plants and highlights how predicted changes in wind patterns may affect vegetation patterns.

Keywords: aeolian processes, airflow modelling, burial, computational fluid dynamics, positive feedback, shading, sub-Antarctic, vegetation patterning.

1. Introduction

Strong and prevailing winds can have considerable effects on the growth and survival patterns of individual plants. The impacts of wind on plants can be direct, by altering a plant's microclimate (e.g. affecting temperature or humidity gradients around leaves) or through mechanical damage to leaves and stems (de Langre, 2008; Grace, 1977; Wilson, 1959). However, the impacts of wind can also be indirect, acting through the entrainment, transport and deposition of particles (Grace, 1977), leading to, for example, erosion around plant's roots, wind-scouring of leaves and stem burial e.g. (Baumeister and Callaway, 2006; Kullman, 2005; van Gardingen et al., 1991). While the direct and indirect impacts of wind on the growth and survival of trees and some crops has been relatively well studied (de Langre, 2008; Ennos, 1997), wind impacts on other growth forms are more poorly understood. Indeed, even though the compact and hemispherical cushion growth form is considered an adaptation to windy conditions (Hauri, 1912) (see also (Hauri and Schröter, 1914) and (Spomer, 1964)), there has been surprisingly little research examining the impact of wind on cushion plants (e.g. (Ashton and Gill, 1965; Fitzgerald and Kirkpatrick, 2017; Lynch and Kirkpatrick, 1995; Whitehead, 1951)).

Cushion plants are often common in cold and exposed areas ((Aubert et al., 2014; Hauri and Schröter, 1914; Körner, 2003)), with the cushion growth form being genetically fixed (i.e. obligate) for many species, but facultative for others i.e. only adopted in windy habitats; (Hauri, 1912; Spomer, 1964). The cushion growth form may also reflect responses to other stressors, such as higher ultraviolet radiations and lower temperatures, which are also prevalent at higher altitudes (Ruffier-Lanche, 1964; Ruthsatz, 1978). In these abiotically-stressful environments individual cushion plants of the same species can exhibit a range of different shapes, particularly as they grow larger (Huntley, 1972; Pyšek and Liška, 1991), despite a circular circumference (i.e. a hemispherical shape) being optimal for heat and moisture retention (Gauslaa, 1984), see also (Zotz et al., 2000). Various mechanisms have been suggested to cause unequal growth and/or mortality on different sides of cushion plants, thereby resulting in the development of non-hemispherical shapes in larger individuals. For example, the presence of rocks and other plants can cause irregular growth of cushions (Pyšek and Liška, 1991), while cushions established on inclines may grow perpendicular to the slope (Selkirk-Bell and Selkirk, 2013; Taylor, 1955a). Turf exfoliation by needle ice formation (in colder areas) and salt-spray deposition (in coastal areas) could also contribute to unequal mortality of cushion plant stems and the development of crescent-shaped cushions (Boelhouwers et al., 2003; Huntley, 1971).

Airflow patterns may also affect the shape of cushion plants (Boelhouwers et al., 2003; Pyšek and Liška, 1991; Whitehead, 1951), as wind strength (i.e. air flow velocity) influences the height, growth rate and compactness of some cushion-forming species (Lynch and Kirkpatrick, 1995) (see also (Fitzgerald and Kirkpatrick, 2017; Huntley, 1972; Ralph, 1978; Ternetz, 1902; Whinam et al., 2014)). The interaction between cushion plant shape and airflow is probably important in exposed sites because plant survival may be strongly linked to the shape of individuals. For example, plants with a more irregular shape offer greater resistance to airflow, and therefore have a greater chance of sustaining wind damage (including breaking of branches and erosion of soil under the plant; (Whitehead, 1951), see also (Cerfonteyn et al., 2011)). As a result, the factors that determine cushion shape probably also affect the survival of individual plants. However, contrasting observations have been made about cushion plants sustaining wind-related damage predominantly on their windward or leeward sides, see e.g. (Ashton and Gill, 1965; Huntley, 1971; Whinam et al., 2014).

Furthermore, because many cushion plant species are nurse plants facilitating the presence of other species, the survival and longevity of cushion plants can considerably alter plant community richness and composition (Badano and Marquet, 2008; Badano and Cavieres, 2006). For example, at high altitudes in the Andes, cushion plants increase local species richness by 22 – 243 % (Badano and Cavieres, 2006) and the biomass of other species by up to 54 % (Badano et al., 2007). Therefore, the pattern of airflow over individual cushion plants may have community-level consequences, directly by providing sheltered establishment sites and indirectly by affecting the survival of the cushion plants and all the species that depend on them. However, apart from a few basic observational studies, see also e.g. (G. M. Courtin and L. C. Bliss, 1971; Wilson, 1959), airflow around cushion plants has yet to be studied in detail.

Due to the differences in the height of origin, mass, density and smoothness of plant seeds and sediment particles, their deposition patterns can differ considerably. In particular, soil sediment particles typically have a relatively high density and are entrained into the airflow from the soil surface (Zhang and Miao, 2003). As a result, sediment particles usually travel close to the ground and for relatively short distances. Wind movement of sediments is well understood, with most sediments accumulating in areas of low shear stress (i.e. regions of decreased velocity) (Durán and Herrmann, 2006; Pye and Tsoar, 1990; Zhang and Miao, 2003). In vegetated areas wind-transported sediments often accumulate on the lee of plants with non-porous canopies or bases that divert airflow (Pye and Tsoar, 1990) or within plants that slow airflow due to a porous canopy (Ravi et al., 2008). Indeed, some species are able to initiate dune (nebkha) formation by causing sand deposition in their lee (Cooke and Warren, 1973).

Here we use computational fluid dynamics techniques to model airflow around cushion plants to predict spatial variation in the direct physical force of the wind and in the accumulation of air-borne seeds, and to understand if these impacts of wind could affect the directional growth and, as a result, the shape of cushion plants. Based on these results, and combined with field observations, we propose a conceptual model of cushion plant shape development in windy environments. In particular we focus on *Azorella selago* (Apiaceae) which is a dominant species across much of the sub-Antarctic (Frenot et al., 1993). The size, shape and compactness of this species are representative of many other cushion plants (Aubert et al., 2014; Rauh, 1939), and it is therefore an appropriate model species for this study.

2. Materials and Methods

2.1. Study species

A. selago (Apiaceae) forms compact cushions with a thin surface layer of photosynthesizing leaves overlying a dense core of live stems, decomposing leaves and fine mineral material soil (Figure 1). Due to their dense nature, cushion plants were modelled as non-porous obstructions to airflow, see e.g.(Hager and Faggi, 1990) . On sub-Antarctic Marion Island (46°54'S, 32°45'E), *A. selago* is the most widespread vascular plant species, and has a median maximum diameter of 0.4 – 1.2 m and a height of 0.05 – 0.20 m, (Huntley, 1972; le Roux and McGeoch, 2004; Phiri et al., 2009) (see also (Chown and Froneman, 2008) for a complete review of the island's climate, geology and ecology).



Figure 1: *Azorella selago* plants on Marion Island with (a) hemispherical shape and (b) crescent shape. A 15 cm length ruler is provided for scale. The grass *Agrostis magellanica* is visible on both cushion plants (see also Fig. 2).

Cushion shape varies between individuals, with smaller plants usually being hemispherical and larger plants having more irregular shapes (Hausmann et al., 2009). Indeed,

larger cushions may often have a crescent shape, with their convex edges facing in the direction of the prevailing wind, i.e. the tails of the crescent point away from the prevailing wind; (Huntley, 1972). As a result, we modelled the airflow over two different plant shapes, corresponding to the size and form of a medium-sized hemispherical cushion and a larger crescent-shaped cushion (sizes based on data from (le Roux and McGeoch, 2004); see Table 1).

Table 1: Model dimensions for cushion plant shapes.

Shape	Plant dimensions [m]		
	Longitudinal diameter	Transverse diameter	Height
Hemisphere	0.3	0.3	0.15
Crescent	0.9	0.4	0.14

The grass *A. magellanica* (Poaceae) is the second most widespread vascular plant on Marion Island (Figure 2; (Huntley, 1971)) and grows both rooted in the soil and epiphytically on *A. selago* (i.e. rooted within the cushion plant's humus-like core) (Huntley, 1972).



Figure 2: *Agrostis magellanica* growing (a) on *Azorella selago* in a fellfield site and (b) in the ground at a low altitude coastal site.

At mid and high altitudes (> 100 m a.s.l.) *A. magellanica* is strongly facilitated by *A. selago*, having higher abundance, cover, biomass and reproductive effort when growing on *A. selago* relative to the adjacent substrate (le Roux and McGeoch, 2010). High densities of

epiphytic *A. magellanica* are thought to have a negative impact on *A. selago* due to the strong shading of the cushion plant's leaves (le Roux et al., 2005), see also (Schöb et al., 2014). At higher altitudes the abundance of *A. magellanica* is thought to be limited by strong winds (le Roux et al., 2005; Taylor, 1955b) see also (Pammenter et al., 1986) and low temperatures (Huntley, 1970).

2.2. Study site: fellfield habitats on eastern Marion Island

Fellfield habitats cover the majority of Marion Island between 100 and 500 m a.s.l. (Smith et al., 2001). This vegetation type is characterised by the dominance of *A. selago* (up to 30 % cover), low total plant cover (usually < 30 %), high rock cover and poorly-developed mineral soils (Huntley, 1971) (Figure 3).

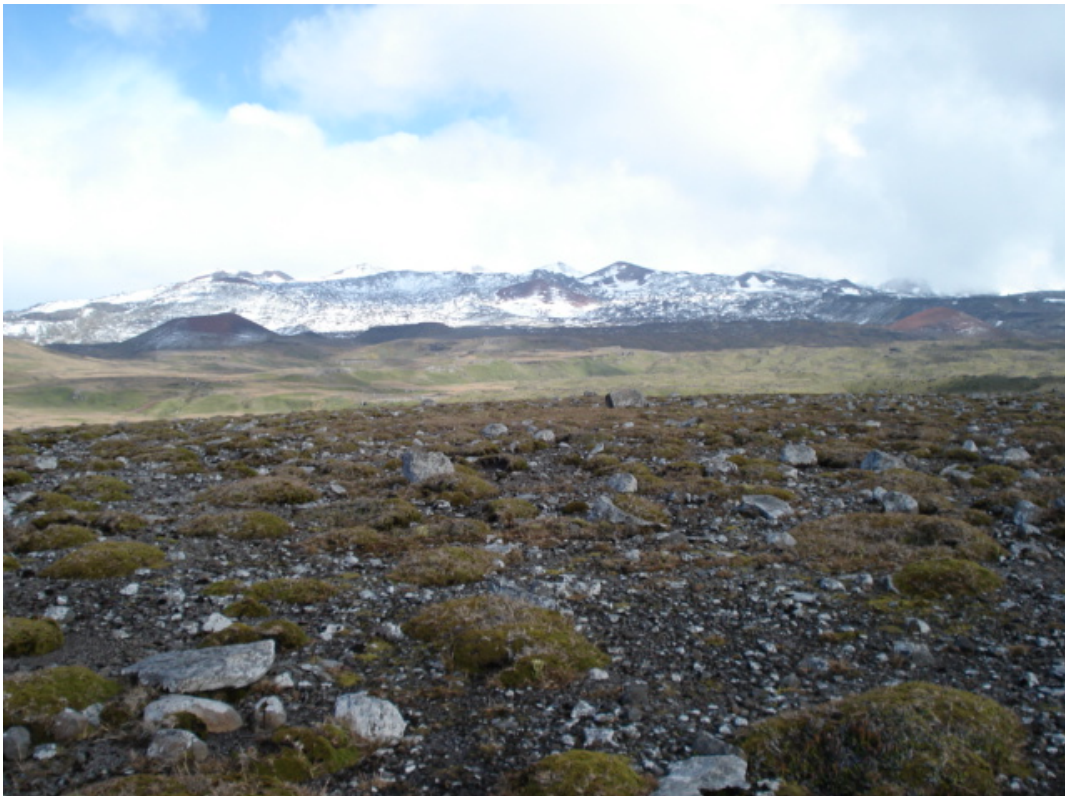


Figure 3: *Azorella selago* and surroundings on Skua Ridge, a fellfield site (c. 100 m a.s.l.).

The climate in these habitats is cold (mean annual temperature = 6.4 °C), oceanic (seasonal temperature range = 4.1 °C) and wet (mean annual precipitation = 1975 mm, mean humidity exceeding 80 %) (data from the meteorological station on the eastern side of the island at sea level; (le Roux, 2008; le Roux and McGeoch, 2008; Smith, 2002)). As is typical for the sub-Antarctic region, the island is very windy, experiencing gale force winds (> 15 m/s) on

more than 100 days per year (Schulze, 1971). The dominant winds on the eastern side of the island are north-westerlies (60 % of observations) and south-westerlies (20 %), which are also the strongest winds, averaging > 10 m/s and 7 m/s respectively (le Roux, 2008). Average wind speed at sea level on the island is 8 m/s, although this is probably stronger at higher altitudes, particularly under neutrally stable atmospheric conditions, (Garratt, 1994); see also le Roux et al. 2018 - 2019 unpublished data, (Berg et al., 2011).

2.3. Modelling airflow using computational fluid dynamics

Previous studies of airflow around plants have almost exclusively considered trees and grasses (de Langre, 2008). Similarly, amongst studies not examining plants, few researchers have documented the patterns of airflow over hemispheres or crescents (Cao and Tamura, 2020; Kim and Baik, 2003; Savory and Toy, 1985; Tavakol et al., 2015, 2010). However, the airflow around spherical and cylindrical obstructions is well described (Achenbach, 1974, 1972; Breuer, 2000, 1998; Constantinescu and Squires, 2004; Dehbi and Martin, 2011; Hoffman, 2006; Lyotard et al., 2007; Norberg, 1987; Raithby and Eckert, 1968; Tiwari et al., 2020), and provides a framework to interpret flow around cushion plants. Indeed, it has been consistently observed that as free-stream air approaches a non-porous bluff (i.e. not streamlined) obstacle, like a sphere or a cylinder, shear forces on the object's surface cause the velocity of the air particles to decrease, creating a narrow boundary layer over the object's surface [i.e. a layer separating the free-stream air and the still air on the obstacle's surface; (Greeley and Iversen, 1985; White, 2016). As air flows over the crest of a cylinder (or around the circumference of a sphere) it attains its highest velocity, and the boundary layer remains relatively thin (Anderson Jr, 2015; Pye and Tsoar, 1990). However, as air particles move into the lee of the obstruction (i.e. downstream of the maximum flow velocity), the boundary layer may separate from the surface of the obstruction due to an adverse pressure gradient [i.e. diminishing of the shear stress, hampering airflow attachment to the plant surface; (Greeley and Iversen, 1985; Houghton and Carpenter, 1993; White, 2016). As a result, a wake forms between the boundary layer and the obstruction, where recirculation occurs (i.e. airflow counter to the free-stream airflow direction), turbulent eddies form and mean air flow velocity is low (Bakić and Perić, 2005; Pye and Tsoar, 1990). Downstream of the obstruction the boundary layer rejoins the surface at the reattachment point, beyond which recirculation is minimal (Pye and Tsoar, 1990).

We investigated these patterns of airflow around hemispherical and crescent-shaped cushion plants growing on a flat surface using computational fluid dynamics (CFD), a

mathematical modelling tool that solves fluid flow problems using numerical algorithms (Versteeg and Malalasekera, 2007). CFD models are based on the three laws of conservation of mass, momentum and energy, from which a system of partial differential equations governing the flow of fluids and entrained particles are derived. These equations are algebraically transformed and solved iteratively. StarCD software (CD-Adapco, London, UK) was used to conduct the airflow analysis over hemispherical and crescent-shaped cushion plant (version 3.24), and to perform Eulerian two phase flow simulations for particle tracks (version 4.06). Complete model specifications, wind tunnel validation and results are provided in (Combrinck, 2009) and verified (Meas et al., n.d.).

In addition to mean airflow patterns, turbulence in atmospheric flow is also well described by the three conservation laws on which CFD modelling is based (see above). However, due to current computational resource limitations, the fine-scale patterns of airflow speed and direction need to be resolved using additional turbulence modelling. A comparison of turbulence models by Combrinck (Combrinck, 2009), based on wind tunnel tests of air flowing over a hemispherical model, concluded that the $k-\varepsilon$ turbulence model (k = turbulence kinetic energy, ε = turbulence kinetic energy dissipation rate) with wall functions can adequately resolve the bulk flow features examined here such as velocity and pressure increase and decrease (Meas et al., n.d.; Versteeg and Malalasekera, 2007).

CFD modelling requires the definition of a computational domain and the specification of boundary conditions (Figure 4). The domain consists of: a free stream velocity inlet with an atmospheric profile (as discussed in section 2.4.1), a pressure outlet, sides and top defined as symmetry planes and no-slip walls with defined surface roughness (discussed in section 2.4.2) to represent the hemisphere or crescent and floor surrounding the cushion.

The computational domain for the hemisphere had a length, width and height of 4 m, 4.5 m and 1.5 m respectively (Table 2). Given the dimensions of the hemisphere (Table 1), the aerodynamic blockage of the hemisphere in the domain was 0.5%, in line with good practice requiring blockage of $< 10\%$ (preventing the boundaries of the domain from influencing the solution). Similarly, the dimensions of the crescent shape computational domain are 5 x 3.5 x 1 m, equating to a blockage percentage of 3.5%. The cell numbers (i.e. the number of units into which the computational domain was divided for calculations) for the hemispherical and crescent shapes were 923 181 and 778 973 respectively. The spatial resolution was constructed for both grid independent and y^+ values associated with the high Reynolds number turbulence model strategy (i.e. y^+ between 30 and 300). Grid independence ensure that the number of units into which the computational domain was divided was sufficiently small to obtain a good

mathematical resolution of the results. Smaller resolutions provide more accurate results, however this comes at the cost of computational time. Part of the verification process of flow modelling is obtaining a grid size that is small enough to obtain a good results within reasonable CPU (central processing unit) time. Another part of verification process was ensuring that the cell size at the walls was appropriate for the turbulence model used. The parameter y^+ is a dimensionless wall distance which is an indication of the cell sizes in the near wall region.

The computational model has to capture the flow physics correctly; this is dependent on the regime of the flow and the solution methodology implemented. The flow was hence defined as incompressible (since the Mach number for air is well below 0.3) with standard atmospheric conditions for the pressure. The simulations were solved in the steady state domain with single precision. The AMG (Algebraic Multigrid) solution method was employed in conjunction with the SIMPLE (Semi-Implicit Method for Pressure Linked Equations) solution algorithm. Discretisation of the domain was done using a central differencing scheme with a blending factor of 0.9. Relaxation factors were employed for the momentum, pressure and turbulent viscosity at values of 0.7, 0.3 and 0.7 respectively. Models were run to convergence where the residual values were both lower than $1e-6$ and stabilised to a near constant value. The hemispherical model converged after 4535 iterations and the crescent shape after 2268.

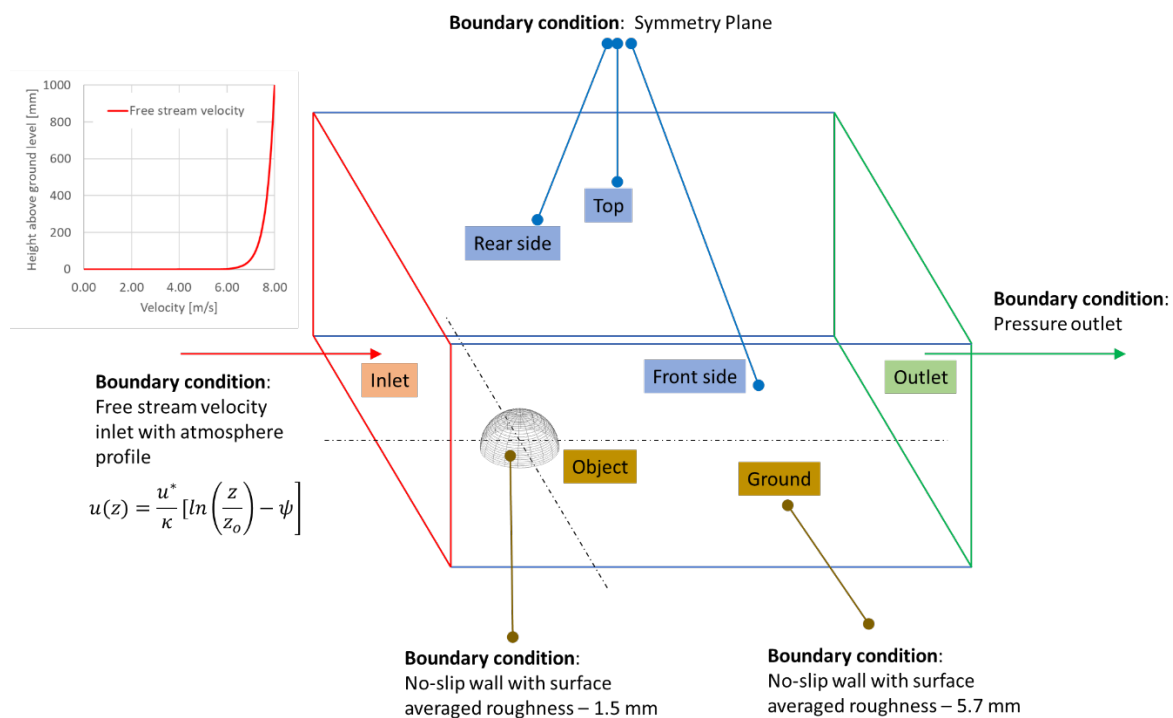


Figure 4: Schematic illustrating the computational domain and boundary conditions. The inset (top-left) illustrates the airflow velocity profile, based on data collected in fellfield vegetation on Marion Island.

Table 2: Model parameters for control volume (the extent over which airflow was modelled).

Shape	Control volume [m]			Blockage %	Cell number	Iterations to convergence
	Length	Width	Height			
Hemisphere	4	4.5	1.5	0.5 %	923 181	4535
Crescent	5	3.5	1	3.6 %	778 973	2268

2.4. Parameterizing the airflow models

First, to simulate airflow over cushion plants, models were parameterized based on the characteristics of *A. selago* cushion plants and on the physical conditions on the eastern side of sub-Antarctic Marion Island in fellfield habitats where the species is the dominant vascular plant. Model parameterization was completed by determining the airflow velocity profile within fellfield habitats, and the surface roughness of *A. selago* cushions and the surrounding surface.

2.4.1. Airflow velocity profile

The vertical airflow velocity profile experienced by *A. selago* cushions was measured in two fellfield sites, Skua-Ridge and Tafelberg, on the eastern side of Marion Island. Wind speed was recorded at three heights (0.20, 0.47 and 1.40 m above the soil surface) using WSD100 anemometers with ± 5 % accuracy and a XR5SE data logger (Pace Scientific, Mooresville, USA; Figure 5).



Figure 5: Measurement setup for airflow velocity profiles (foreground) near the Marion Island base (background).

Data were obtained on Skua-Ridge on three different days measuring one sample per minute for three hours. On Tafelberg this was repeated also on three separate days taking four samples per minute for 1.5 hours. Airflow velocity increased strongly with height (Table 3), and a logarithmic relationship fitted the data well ($R^2 = 0.98 - 0.99$, $p < 0.001$) for both sites after log-transformation.

Table 3: Mean airflow velocity in fellfield habitats on the eastern side of Marion Island.

Height above the soil surface (m)	Airflow velocity [m/s] (mean \pm S.E.)	
	Site 1: Skua-Ridge (± 100 m a.s.l.) ¹ n = 540	Site 2: Tafelberg (± 300 m a.s.l.) ² n = 1080
0.20	6.36 \pm 1.32	6.53 \pm 1.10
0.47	7.64 \pm 1.53	7.76 \pm 1.35
1.40	9.84 \pm 1.82	9.85 \pm 1.61

¹ n = 540, one measurement per minute for three hours, repeated on three different days; ² n = 1080, four measurements per minute for 1.5 hours, repeated on three different days.

As a result, the airflow velocity profile was modelled by:

$$u(z) = \frac{u^*}{\kappa} \left[\ln \left(\frac{z}{z_0} \right) - \psi \right] \quad (2)$$

where u^* is the friction velocity, κ is the von Kármán constant (= 0.41), z is the height above the soil surface and z_0 the roughness length (following (Petersen et al., 1998)). The final parameter, ψ , is a stability-dependent function that is positive in unstable conditions, negative in stable conditions and zero for neutral stability (Kim and Baik, 2003; Petersen et al., 1998; Yang et al., 2008). To achieve a logarithmic vertical airflow profile (such a observed in the result shown in ?) with a mean velocity of 8 m/sec at 1.5 m height (i.e. the mean speed recorded at the island's meteorological station (le Roux and McGeoch, 2008)) over a surface with $z_0 = 0.0057$, we set $u^* = 0.138$ and $\psi = -18$. This vertical airflow velocity profile was then used in all simulations.

2.4.2. Surface roughness parameters

Both Skua Ridge and Tafelberg are pre-glacial lava flows dominated by smooth basalt rocks. The sediment size in the immediate surface area around *A. selago* can display a high degree of variation (e.g. Figure 6).



Figure 6: Sediment surrounding *Azorella selago* indicating (a) high variability and (b) low variability in size.

The diameter of surface particles around *A. selago* cushions at a fellfield site on the eastern side of Marion Island ranged between 2.0 and 313.2 mm (Hausmann et al., 2009). The mean particle size (5.7 mm diameter) was therefore used as an estimate of ground surface roughness. The surface roughness of fellfield *A. selago* cushions was estimated as 1.5 mm (pers. obs.; MLC), reflecting the average deviation of the height of the leaf surface.

The model for surface roughness in StarCD version 3.24 is based on the sand grain experiments of Nikuradse (H. Schlichting, 1968). The modified Law-of-the-Wall equation is used to model fully rough walls at high Reynolds numbers:

$$u^+ = A + \frac{1}{\kappa} \ln \left(\frac{y^+ - D^+}{B + CR^+} \right)$$

where

$$D^+ = \rho C_\mu^{0.25} k^{0.5} \frac{D}{\mu} \tag{1}$$

$$R^+ = \rho C_\mu^{0.25} k^{0.5} \frac{y_0}{\mu}$$

The generic values for the constants A, B, C, D and C_μ are 8.5, 0, 1, 0 and 0.09 respectively. κ is the von Kármán constant (= 0.41). The parameter y_0 represents the roughness height; this was specified in the model as 5.7 mm and 1.5 mm for the ground and plant area respectively.

2.5. Modelling seed deposition

The deposition of solid particles on cushion plants was modelled using a Eulerian two phase flow model, where Phase 1 represents the continuous fluid (i.e. the airflow) and Phase 2 the dispersed particles (i.e. seeds) (CD-Adapco Group, 2008). The two phases (a gas and a

solid) behave differently in the proximity of an obstruction due to their different physical properties and densities. In particular, while the trajectory of an air particle is deflected by an object (guided around the curvatures), a solid particle is more likely to impact with the obstruction (due to the greater momentum of heavier particles; (CD-Adapco Group, 2008)). In contrast to sediment particles, seeds are lighter (equivalent to airborne contaminants in CFD modelling; (CD-Adapco Group, 2008)) and are released into the airstream above the ground surface (e.g. inflorescences at 0.05 – 0.4 m in fellfield; le Roux et al. unpublished data).

Seed particles in the model were parameterized based on the aerodynamic characteristics of the seeds of the common grass *Agrostis magellanica*. The seeds appear to be dispersed within their spikelets, which have an irregular shape and numerous sharp points, which are likely to enhance seed adherence to surfaces. As a result, the seeds (and the spikelets) are likely to be deposited on first impact, while smoother sediment particles are more likely to be deflected and only settle in low airflow velocity conditions, see also (Beyers and Waechter, 2008; Grace, 1977). Therefore, air-borne seeds and sediment are expected to have different deposition patterns due to differences in their mass, shape and the height at which they are entrained into the airstream. As sediment deposition has been modelled extensively in other studies, seed deposition was the focus of this study.

The mean drag coefficient of *A. magellanica* seeds was determined using a gravitational drop test (Combrinck, 2009; C.T. Crowe et al., 2001), where the mean time taken for seeds to fall 4.15 m was determined. *A. magellanica* inflorescences were collected from the eastern side of the island, and dried at room temperature. Individual spikelets ($n = 150$) were separated from the inflorescence, weighed (mean \pm S.E. = 0.29 ± 0.09 mg) and measured (mean \pm S.E. maximum diameter = 3.26 ± 0.09 mm). For calculations the assumption was made that seeds instantly reached terminal velocity [see (Grace, 1977), data analysed in Matlab version R2007b, details in (Combrinck, 2009)]. The average time of first arrival (3.33 sec) was used, excluding seeds which fell more slowly due to collisions with the container wall during descent. Four equations were used to model the drag coefficient of the seeds (Clift and Gauvin, 1970; Flemmer and Banks, 1986; Perry and Chilton, 1973; Schiller and Naumann, 1933), of which the Flemmer and Banks correlation (Flemmer and Banks, 1986) had the smallest difference between the numerical and experimental drag coefficient. As a result, the drag coefficient calculated by this method ($C_d = 0.681$) was considered most suitable for this application, within the range of values reported by e.g. (Greene and Quesada, 2005).

In the CFD simulations the deposition of seeds on *A. selago* plants was modelled by releasing particles at the air inlet of the computational domain (Figure 4) with a volume fraction

of 0.01% in the dispersed phase (Phase 2). The seeds were assumed to be spherical particles with a diameter of 3 mm. The virtual mass was left per default value of 0.5. The drag coefficient was specified as 0.681.

3. Results

3.1. Airflow patterns

Results are displayed through contour plots of velocity magnitude (using side and top views at various slices through the computational domain), velocity vector plots (to highlight regions of recirculation and reattachment), air particle tracks (to show the path of a particle though the domain), pressure contours on the hemisphere or crescent and velocity profiles extracted at specified points (Figure 8, Figure 9). Figure 7 facilitate explanation of the flow results obtained from the CFD analysis. In each image the flow direction is indicated along with the orientation from which it is shown (i.e. top view or front view and x-y-z axis orientation). This convention is used consistently throughout the manuscript.

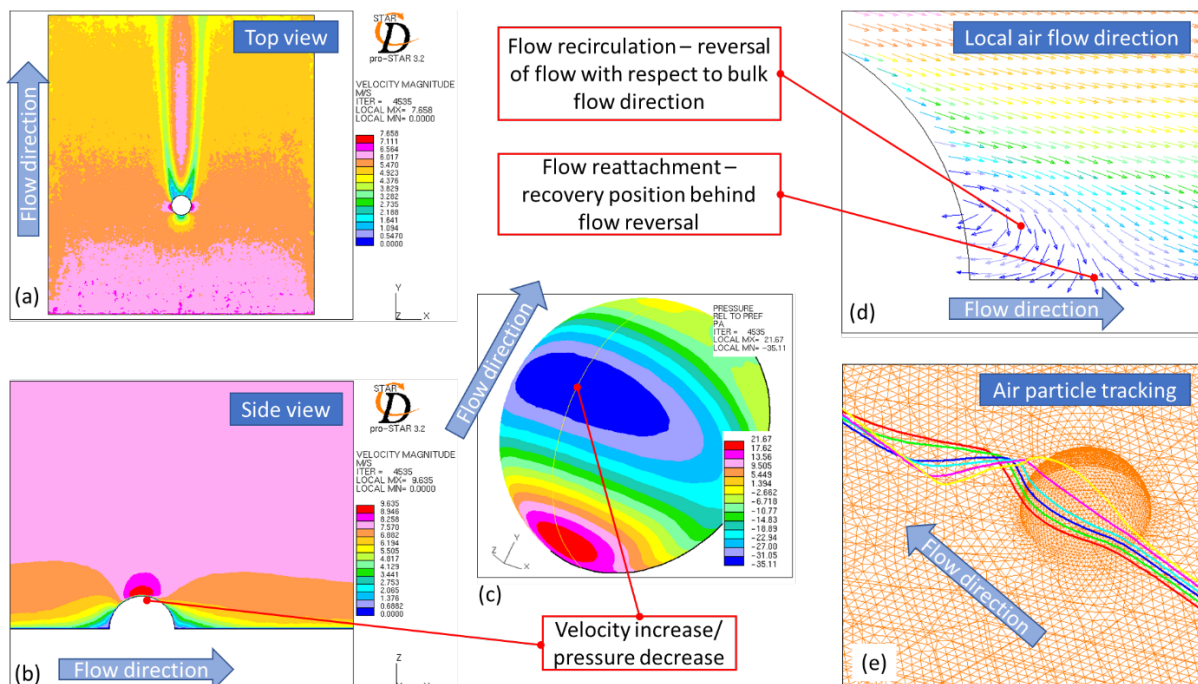


Figure 7: Explanatory image of the view orientation and flow direction of CFD results.

Vertical velocity profiles were obtained at the midsection of the hemisphere and crescent shape, this extended from the ground level to the top boundary of the domain (Figure 8). The data from four sample lines were extracted; directly in front, at the apex,

directly behind and 0.4 m behind the object. The results are displayed in (Figure 9); this is used in subsequent paragraphs to describe the behaviour of the airflow.

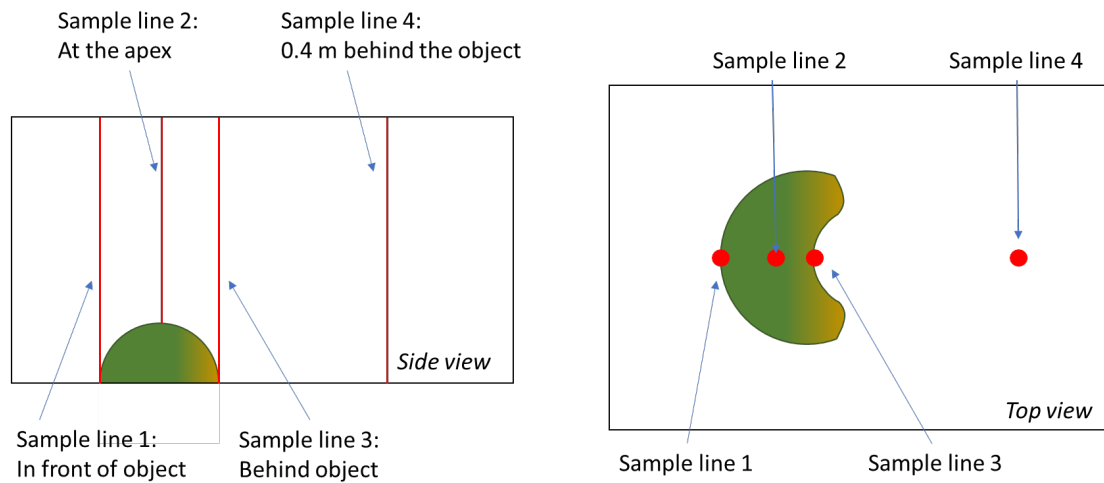
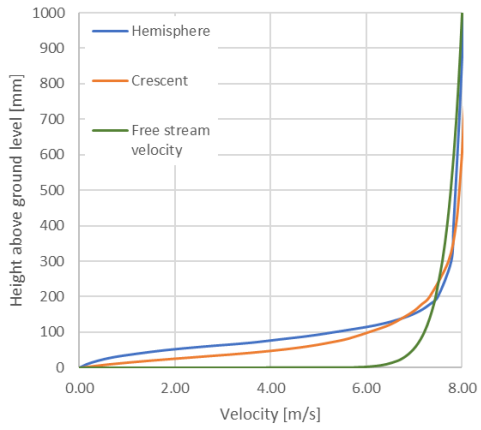
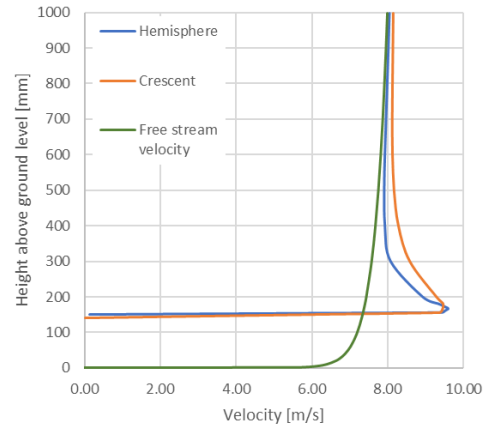


Figure 8: Sample lines in the computational domain where velocity profiles were extracted.

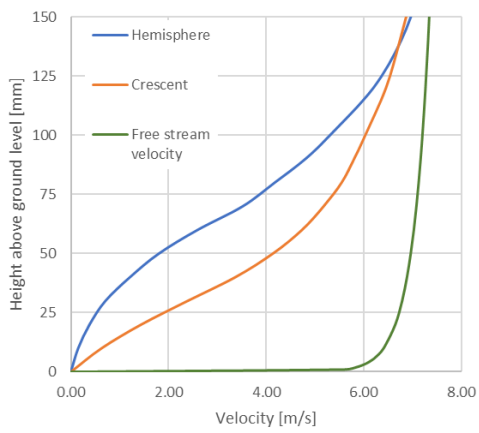
In the analyses of the hemisphere the airflow decelerated at the leading edge (from Figure 9 velocities were 1.2 m/s, 4.17 m/s and 6.18 m/s directly in front of the hemisphere at heights of 40 mm, 80 mm and 120 mm respectively, in comparison with free stream velocities of 6.88 m/s, 7.12 m/s and 7.26 m/s at similar heights) of the cushion plant. This created a region of high pressure approximately 21.67 Pa higher than the reference atmospheric pressure; 101 350 Pa. The flow was deflected equally over and around the plant (Figure 10, Figure 11). As a result, faster air flow (maximum velocity was 10 mm above the apex of the plant at 9.42 m/s) and lower pressure following Bernoulli's principal (35.11 Pa lower than the reference pressure) occurred over the top and around the sides of the plant (Figure 12). This suggests that wind scouring would be greatest on these portions of the cushions' windward aspect. In the lee of the hemispherical cushion plant airflow velocity was slower in two narrow zones, separated by a broader region of airflow at the midsection of the domain (from Figure 9 the flow directly behind the plant was 1.75 m/s, 3. 89 m/s and 6.38 m/s at heights of 40 mm, 80 mm and 120 mm respectively, in comparison with free stream velocities of 6.88 m/s, 7.12 m/s and 7.26 m/s). This pattern of three trailing zones of airflow velocity suggests the establishment of a horseshoe vortex in the lee of hemispherical plants (Figure 13), which regularly sheds vortices (i.e. turbulent eddy features comprising recirculating air) in two distinct areas. Therefore, under average wind speed conditions, two lines of eddies form behind hemispherical cushion plants.



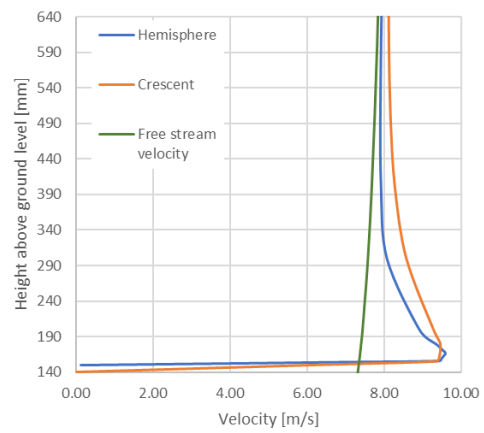
(a)



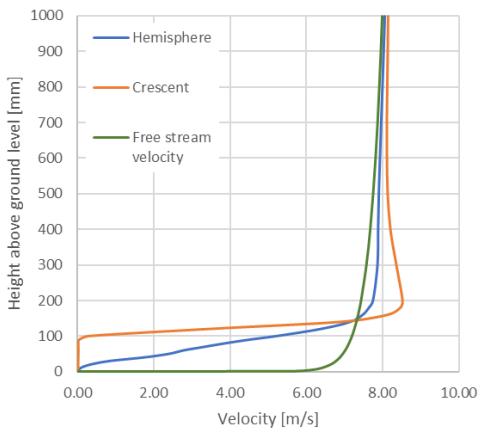
(d)



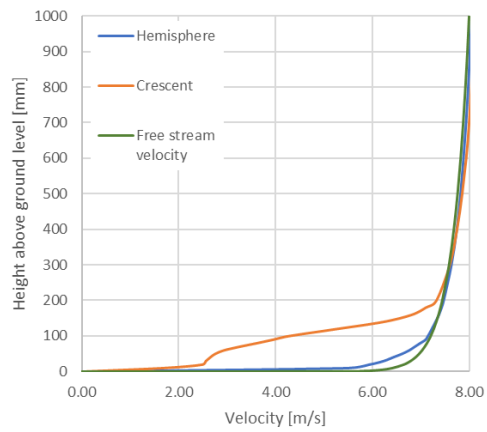
(b)



(e)



(c)



(f)

Figure 9: Comparison of velocity profiles for hemispherical and crescent shapes at (a)&(b) directly in front (sample line 1), (c) at the apex (sample line 2), (d)&(e) directly behind (sample line 3) and (f) 0.4 m downwind of the plant (sample line 4).

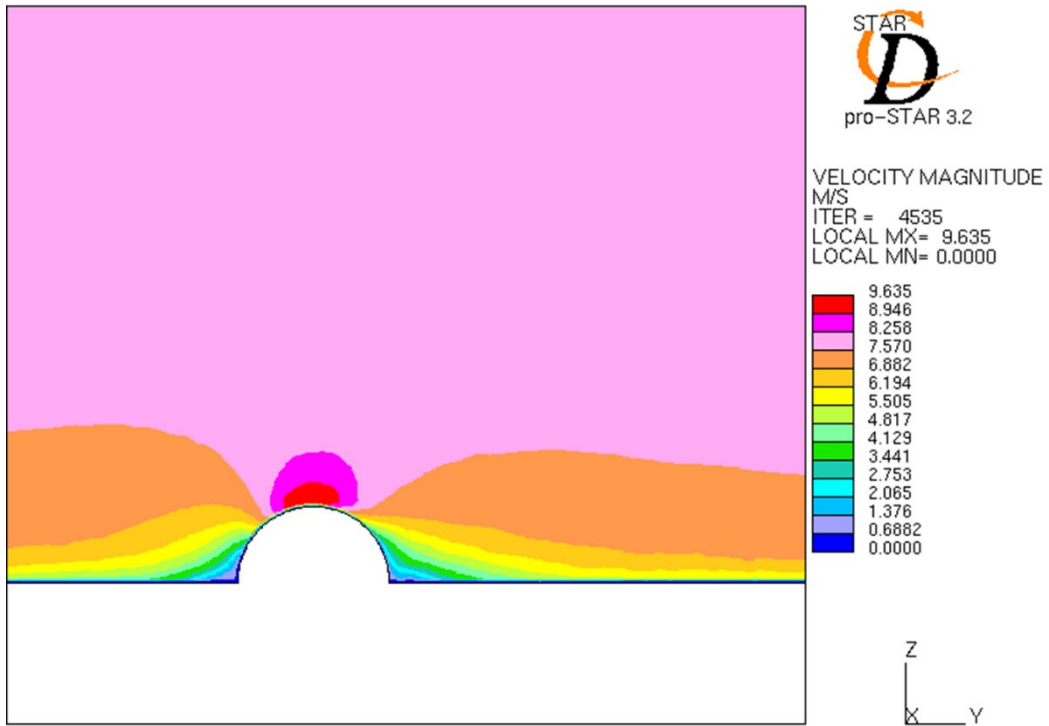


Figure 10: Airflow velocity magnitude around hemispherical shape; side view taken at the midsection.

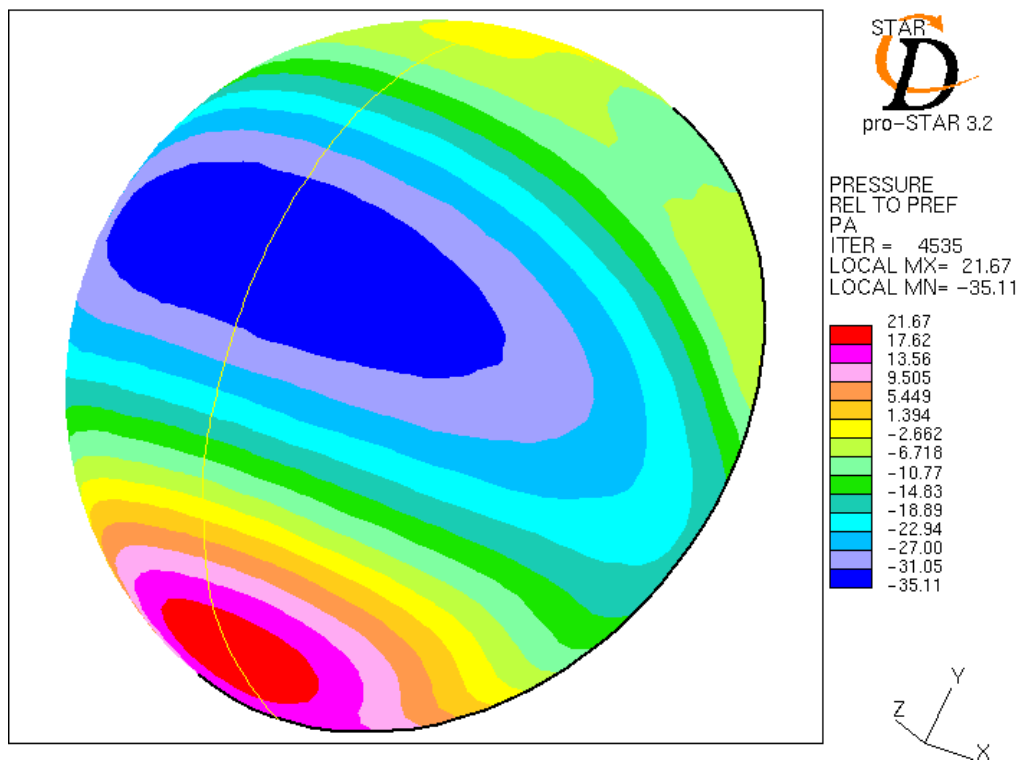


Figure 11: Pressure contours over the hemispherical shape relative to atmospheric pressure.

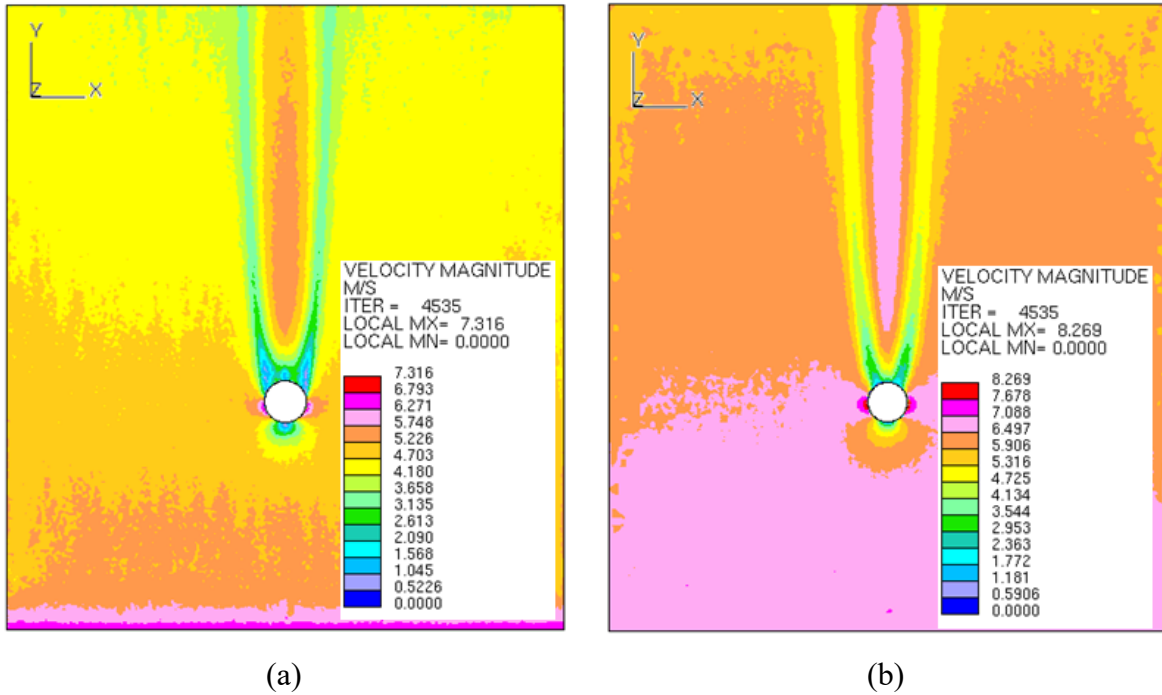


Figure 12: Airflow velocity magnitude around hemispherical shape; top view taken at (a) 7.5 mm and (b) 49.5 mm from the ground level.

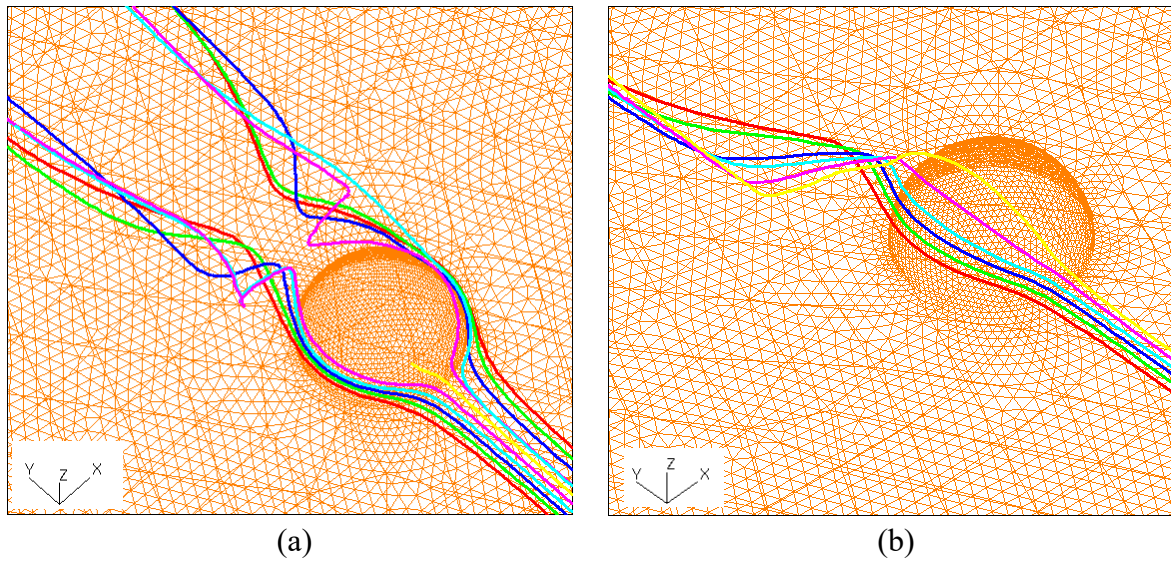


Figure 13: Air particle path line for arrival at the hemispherical shape (a) 20 mm and (b) 30 mm from ground level.

On the windward side of hemispherical cushions airflow closely followed the contours of the plant (e.g. Figure 13). However, in the plant's lee, airflow separated from the plant's surface and started to recirculate, forming a wake (Figure 14, Figure 15). Airflow only became more regular (and recirculation reduced) well beyond the trailing edge of the plant, with the distance to airflow reattachment varying with distance from the center of the plant (Figure 16). The distance to airflow reattachment was greater further from the mid-plane of the cushion (i.e.

stronger recirculation occurring further from the center of the cushion within the two trailing zones of lower airflow velocity). As a result, recirculation was reduced behind the center of the plant relative to its edges (Figure 17). Recirculation was strongest close to the ground but weaker higher above the ground surface (Combrinck, 2009).

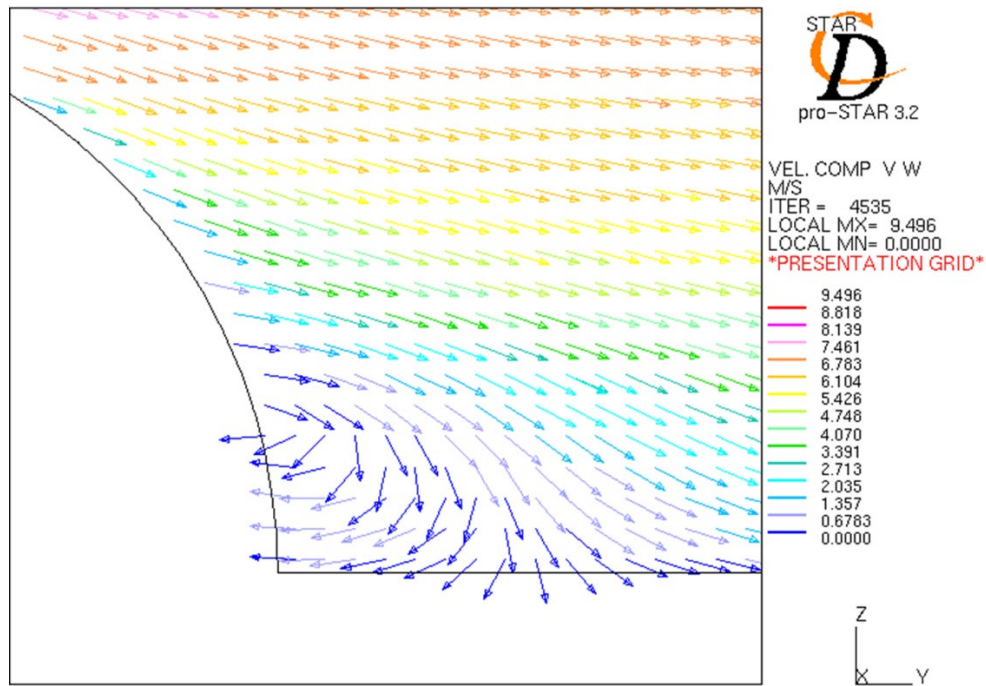


Figure 14: Velocity component direction (Y-Z) at a vertical plane 64 mm from the hemisphere midsection.

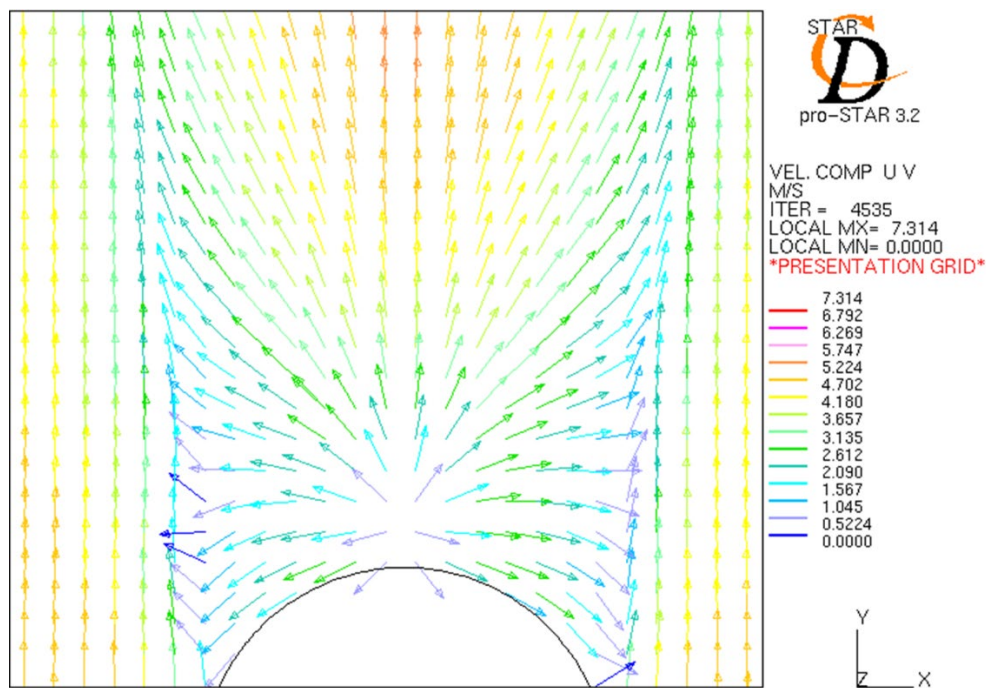


Figure 15: Velocity component direction (X-Y) at a horizontal plane 7.5 mm from the hemisphere ground level.

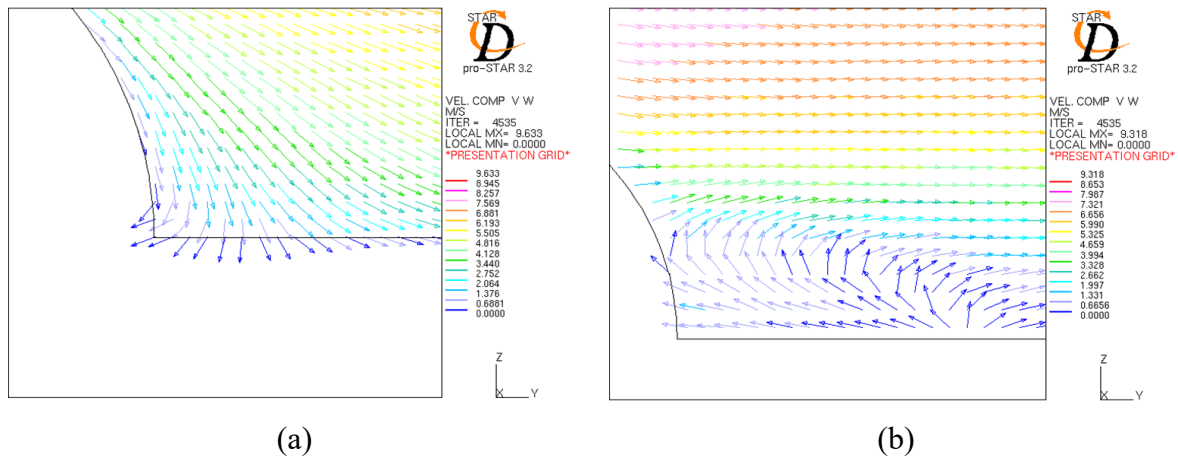


Figure 16: Velocity component direction (Y-Z) at a vertical plane (a) at the midsection and (b) 88 mm from the hemisphere midsection.

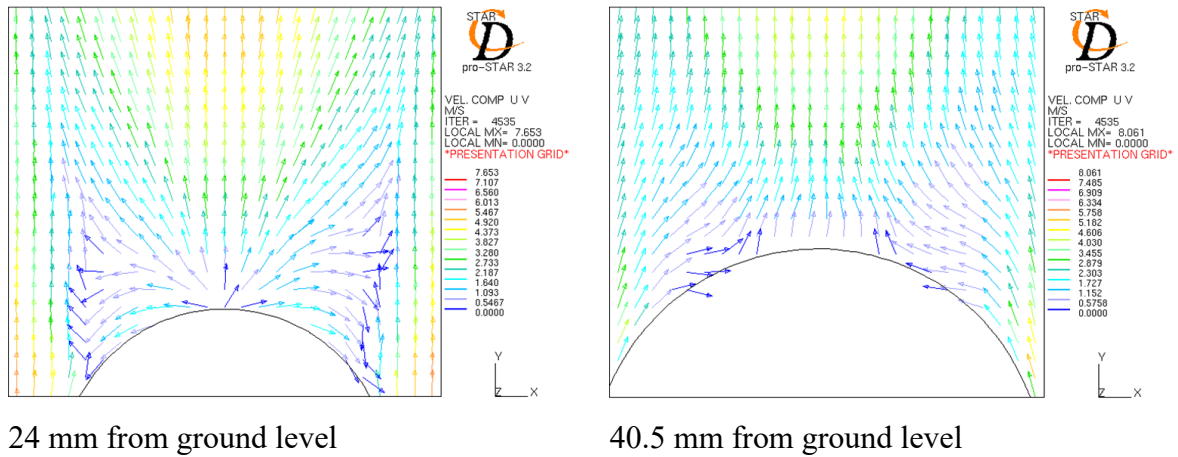


Figure 17: Velocity component direction (X-Y) at a horizontal plane (a) 24 mm and (b) 40.5 mm from the hemisphere ground level.

Airflow patterns were similar on the windward sides of the crescent and the hemispherical cushion plants, with a deceleration of air velocity (from Figure 9 velocities were 3.36 m/s, 5.54 m/s and 6.45 m/s directly in front of the hemisphere at heights of 40 mm, 80 mm and 120 mm respectively, in comparison with free stream velocities of 6.88 m/s, 7.12 m/s and 7.26 m/s at similar heights) in front of the crescent cushion due to the obstruction of the airflow (Figure 18). This resulted in a zone of high pressure (14.76 Pa higher than the reference atmospheric pressure; 101 350 Pa) along the leading edge of the plant (Figure 19). On the sides and the top of the plant the airflow accelerated and a distinct area of low pressure was formed (maximum velocity of 9.35 m/s was reached approximately 15 mm above the plant apex at a pressure of 33.6 Pa lower than reference pressure) (Figure 19). On the leeward side of the plant the airflow showed three areas of differing velocities, with the lowest velocity in the center, bordered by two trailing zones of slightly accelerated airflow (Figure 20). There is a distinct

region of near zero velocity flow directly behind the plant the extends to approximately 90 mm above ground level (Figure 9). The low velocity flow extends to 120 mm above ground level where the velocity is 3.45 m/s, the free stream in comparison at that height would have been 7.26 m/s. While the two outer zones (faster airflow, Figure 20) weaken rapidly with increasing height, the central zone of slower mean airflow weakened more slowly. The central zone of airflow therefore represents a single vortex street being shed in the wake of the crescent (Figure 21), contrasting with the horseshoe vortex observed behind hemispherical cushion plants.

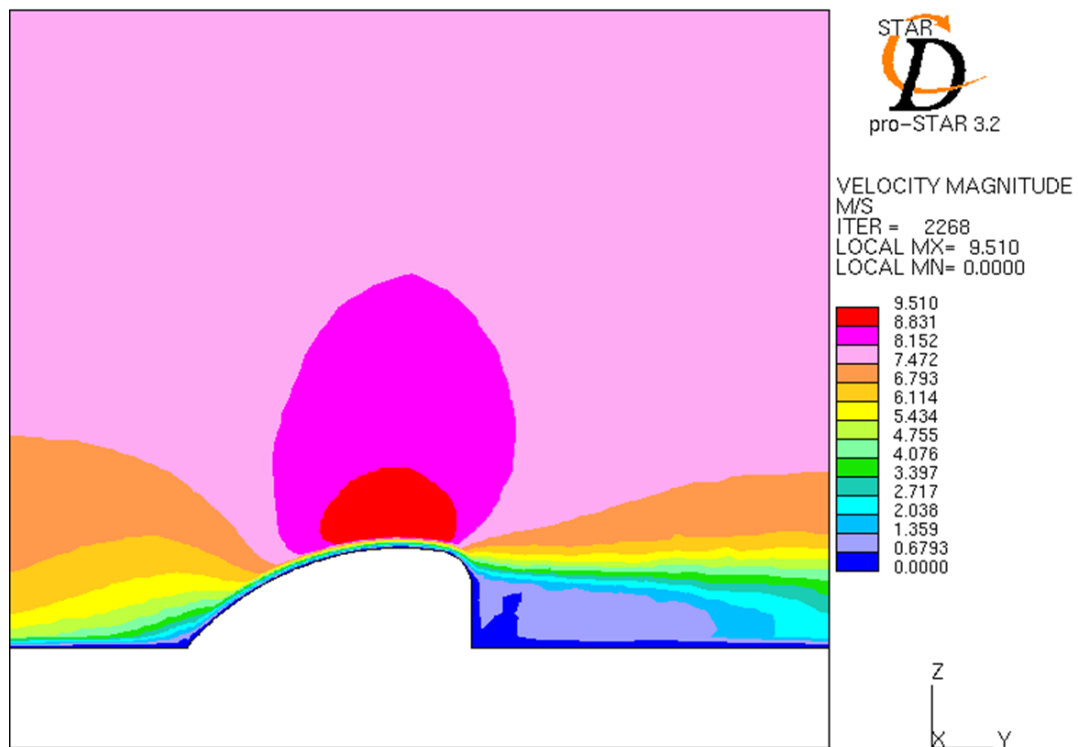


Figure 18: Airflow velocity magnitude around crescent shape; side view taken at the midsection.

Recirculation patterns in the lee of the crescent cushion were more pronounced, and of a different form, than those behind the hemispherical plant (Figure 22, Figure 23). The ground level airflow around the crescent was pulled into the recirculation zone behind the plant, and then directed upwards (Figure 24). Additionally, in contrast to the hemispherical plants, the distance to airflow reattachment was further from the center of the plant than from the edges of the cushion (Figure 25) illustrating the persistence of turbulence due to the vortex street in the lee of the plant.

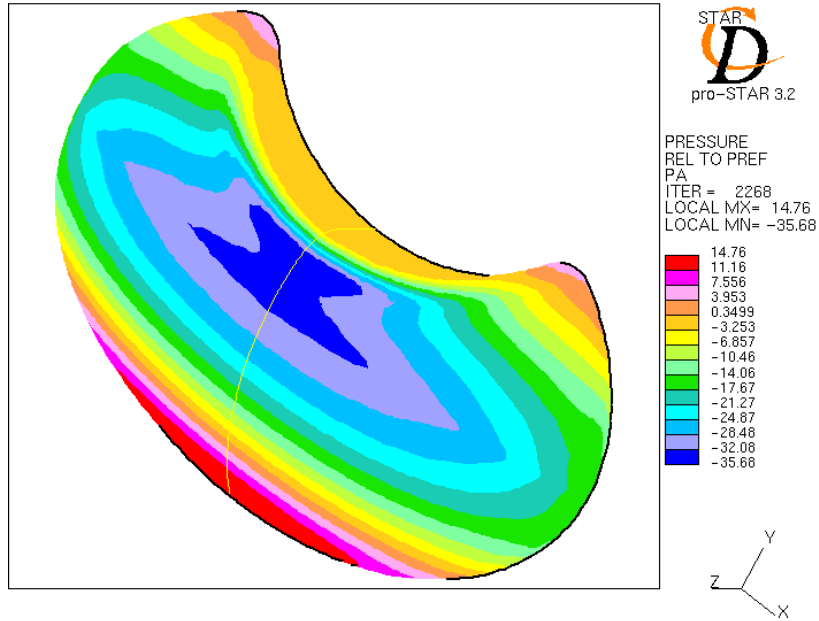


Figure 19: Pressure contours over the crescent shape relative to atmospheric pressure.

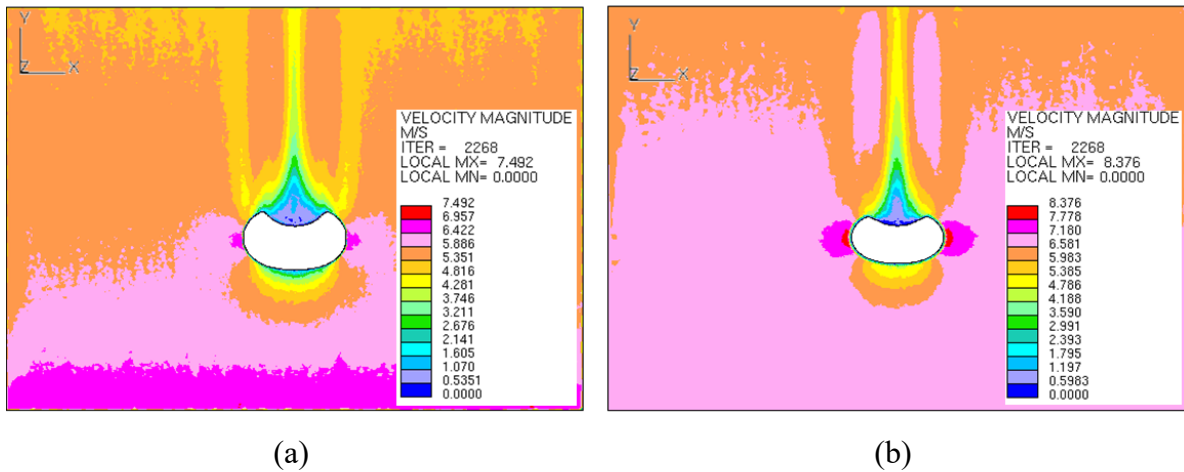


Figure 20: Airflow velocity magnitude around crescent shape; top view taken at (a) 16 mm and (b) 55 mm from the ground level.

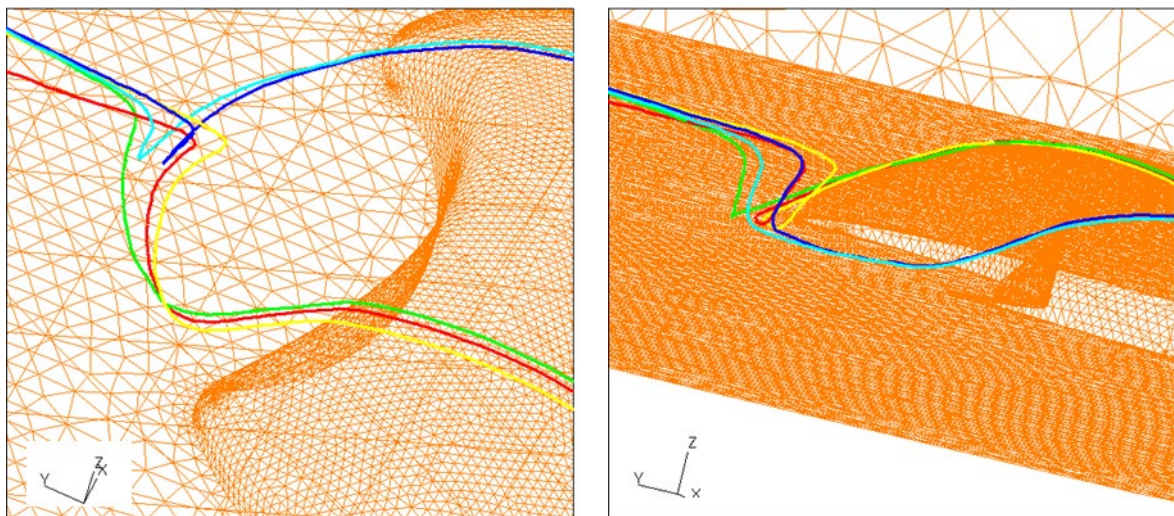


Figure 21: Air particle path line for arrival at the crescent shape 2 mm from ground level.

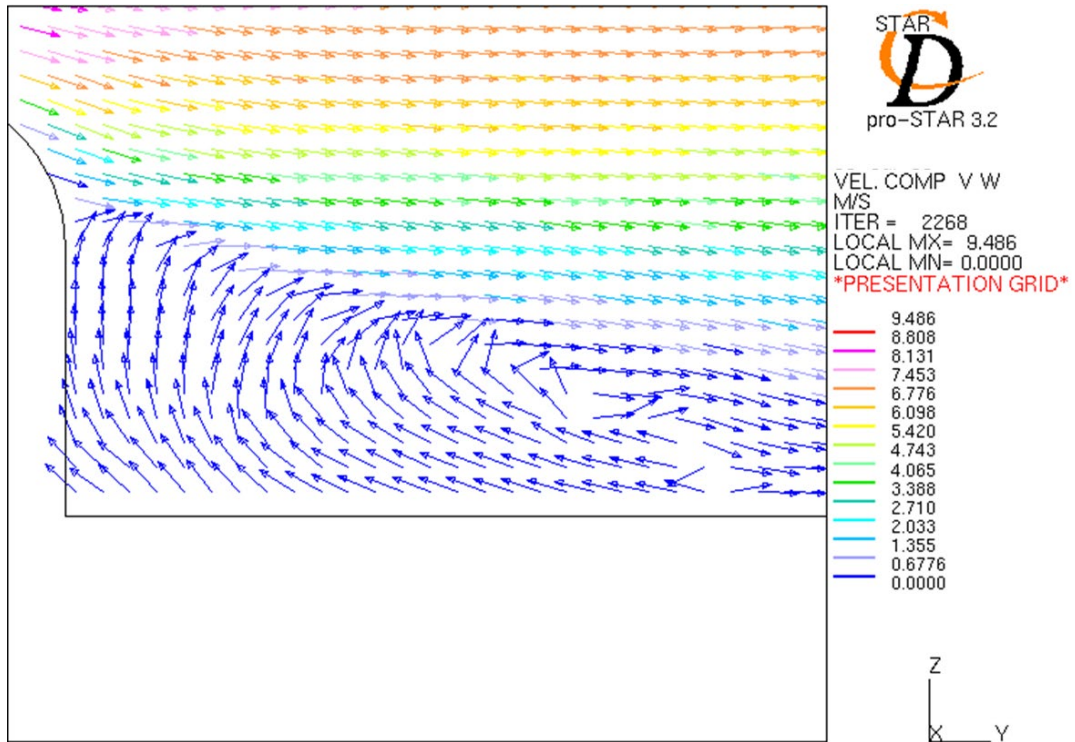


Figure 22: Velocity component direction (Y-Z) at a vertical plane 55 mm from the crescent midsection.

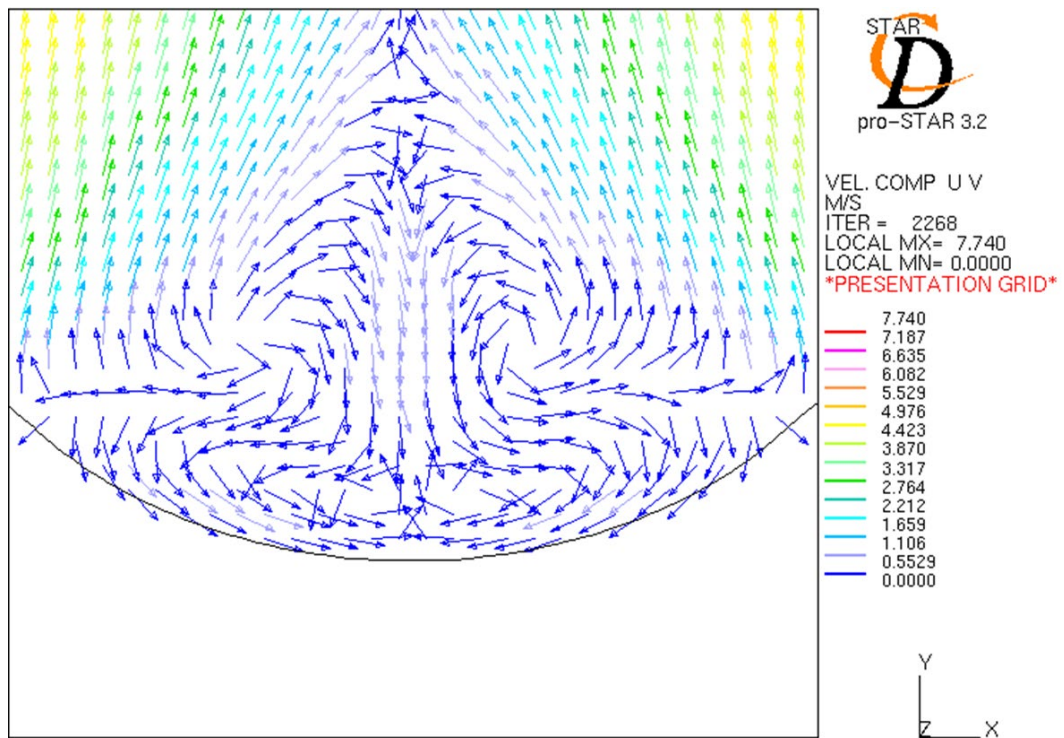


Figure 23: Velocity component direction (X-Y) at a horizontal plane 22 mm from the crescent ground level.

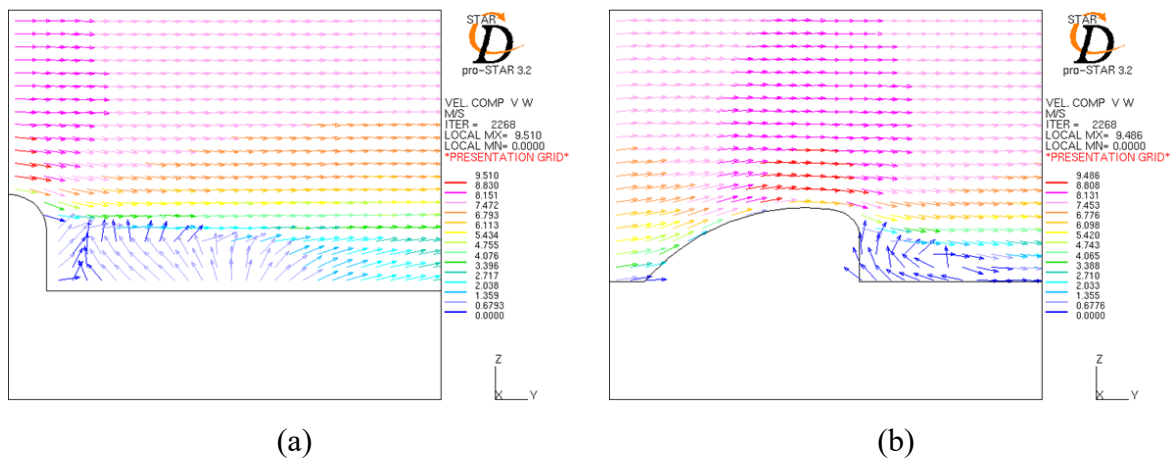


Figure 24: Velocity component direction (Y-Z) at a vertical plane (a) at the midsection and (b) 55 mm from the crescent midsection.

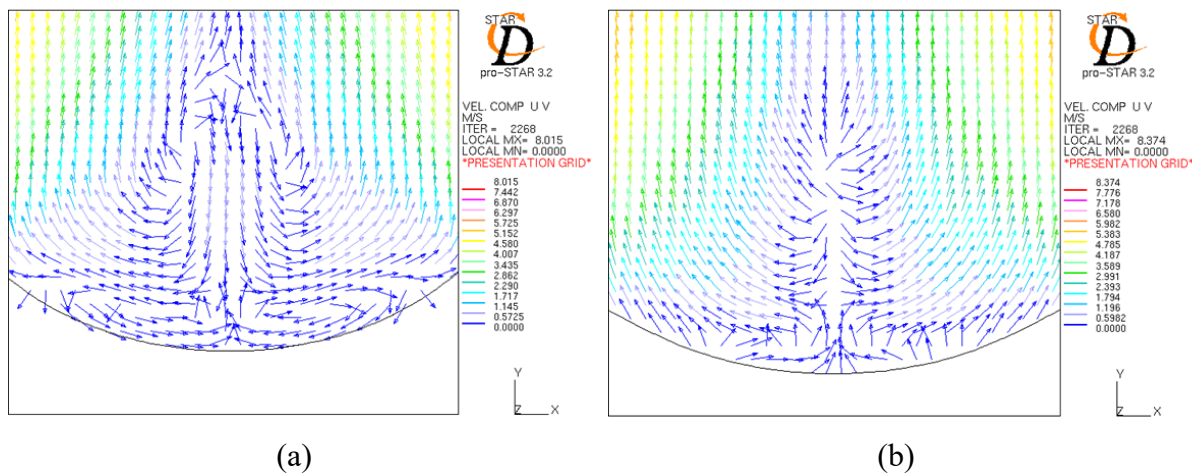


Figure 25: Velocity component direction (X-Y) at a horizontal plane (a) 33 mm and (b) 55 mm from the hemisphere ground level.

3.2. Seed deposition

The flow patterns between the continuous phase (Phase 1, airflow modelled as a gas) and the dispersed phase (Phase 2, seeds modelled as solid particles) is distinctly different (Figure 26). The recirculation patterns behind the hemispherical and crescent shapes are also less complex for Phase 2 than observed for Phase 1 in the previous section.

An air particle is deflected over and around the sides of the object, guiding it along the curvatures and forming unique patterns such as the horseshoe vortex behind the hemisphere. The entrained solid particle has a greater mass and will be propelled by its momentum in the air stream. An entrained seed approaching an obstacle will behave in a number of ways; it may impact with the object on the windward side or it may be carried upwards or around the sides of the object with the air stream. It was previously explained that seed are likely to deposit on the plant at first impact due to their irregular shape and numerous sharp points. Therefore,

seeds that impact on the windward side is not expected to be displaced to other regions of the plant. In the second instance where the seed was lifted over and deflected around the plant the momentum imposed on the seed by the increase of the airflow in this region will likely carry it away from the plant. A portion of the seeds lifted and deflected, that is not displaced by momentum, will be further entrained by the airflow and trapped in the recirculation region. It is expected that these seeds will be deposited on the lower regions of the leeward side of the plant where it is sheltered from the elements thus facilitating germination.

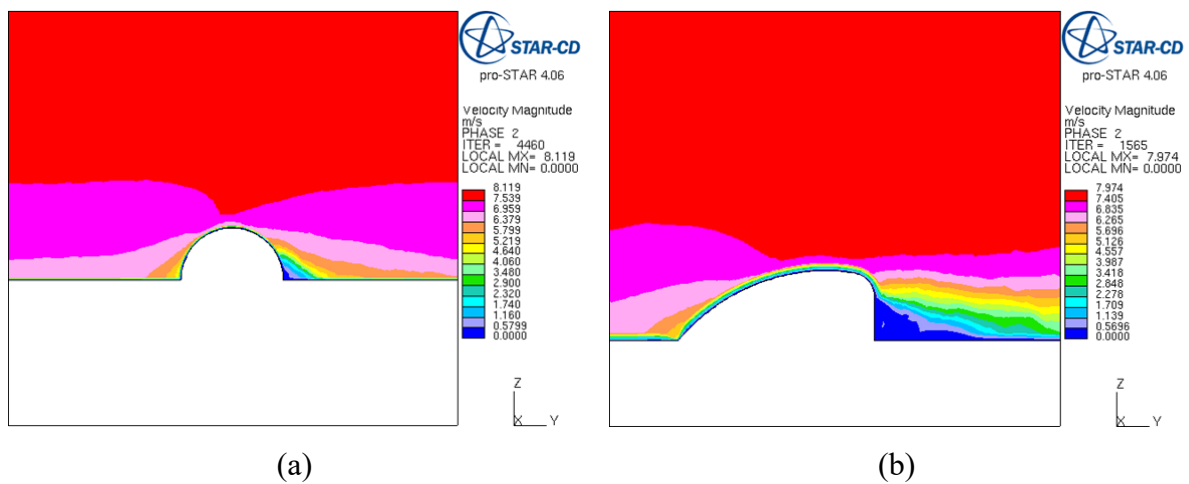


Figure 26: Velocity of entrained light particles (i.e. seeds) in the vicinity of (a) hemispherical and (b) crescent shaped plants.

Simulations suggest that most seeds would be deposited in the upper middle region of the windward side of cushion plants (red region in Figure 27 and Figure 28), suggesting that the friction drag forces of the air on the seeds particles were insufficient to lift a significant portion of the seeds over and around the plant. However, in the regions closer to the ground a portion of the seeds were carried upwards and deposition in the region indicated in red. Accelerated airflow on the sides and the top of the plants increased the momentum and kinetic energy of the seeds, causing them to deflect from the plant in the direction of the resultant residual forces. Therefore, few particles were deposited on the leeward side of the plant through the mechanism of recirculation in the flow field. However, because light particle recirculation extended to a height of 39 mm (Figure 29) for hemispherical cushion and to 81 mm (Figure 30) for crescent plants (both plants having similar heights; Table 1), a greater proportion of particles were deposited on the leeward side of the crescent-shaped plants than on the leeward side of the hemispherical plants.

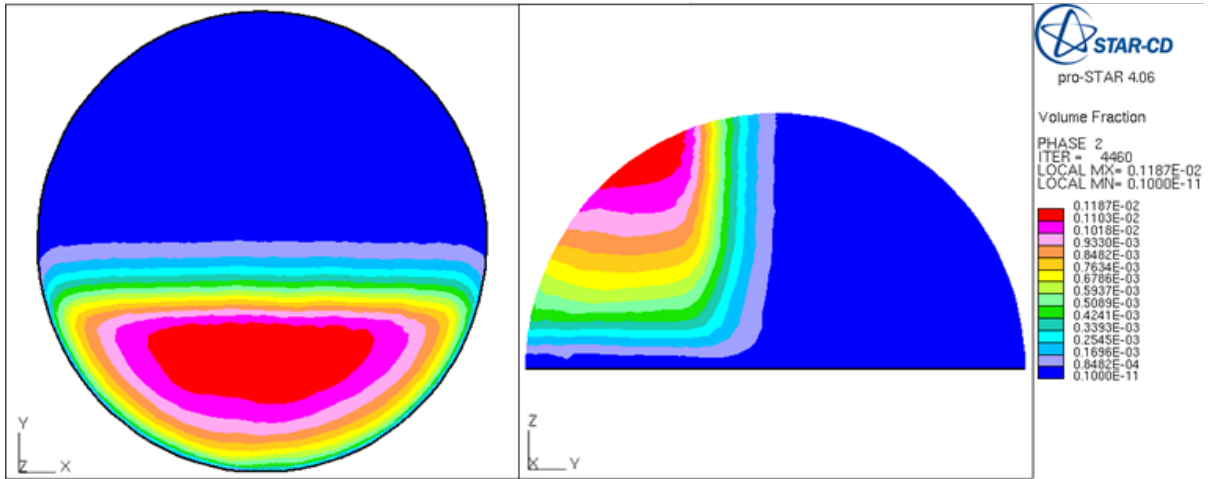


Figure 27: Volume fraction of seed particle deposition on hemisphere

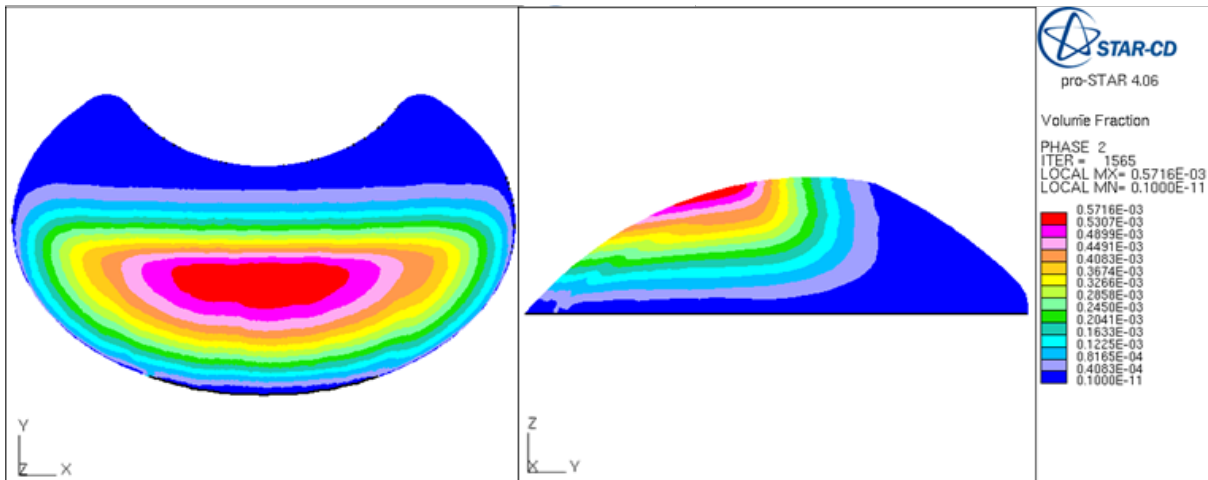


Figure 28: Volume fraction of seed particle deposition on the crescent

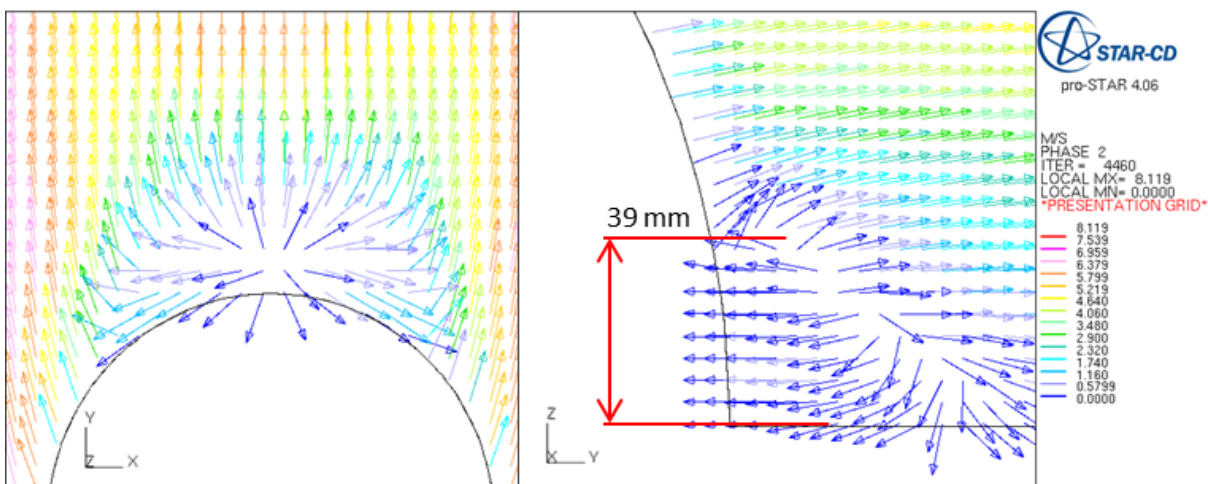


Figure 29: Velocity vectors of entrained light particles (i.e. seeds) around the hemisphere indicating the height of recirculation above ground level (39 mm).

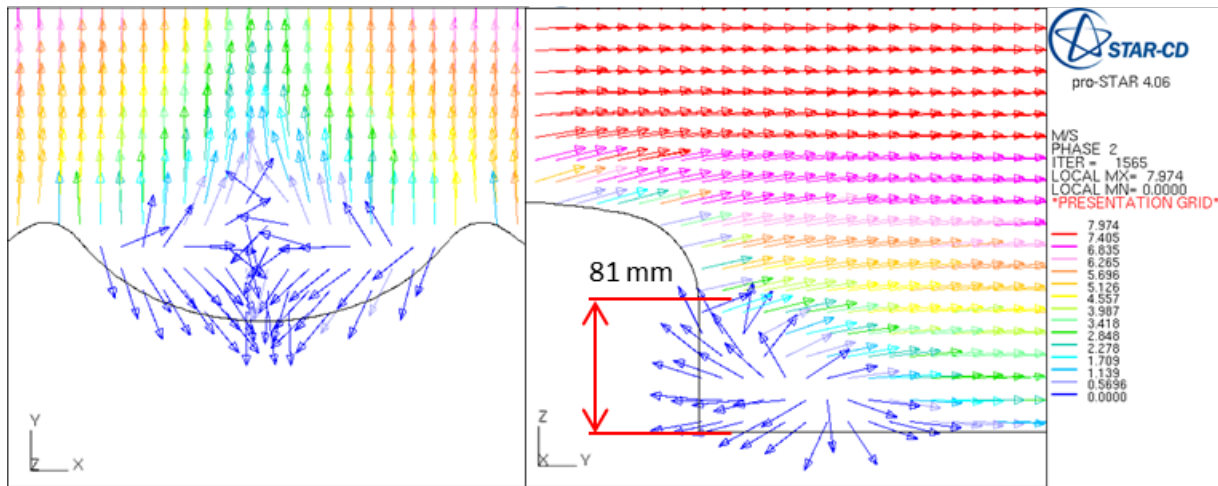


Figure 30: Velocity vectors of entrained light particles (i.e. seeds) around the crescent indicating the height of recirculation above ground level (81 mm).

The mathematical simulation of airflow around different shapes of cushion plants provided a clear indication of the potential impacts of wind on these plants. Numerical analyses indicated some similarities in airflow velocity patterns around hemispherical and crescent-shaped plants. For example, air velocity was always fastest on the top and sides of the plants, with the highest air pressure on their windward sides (suggesting the greatest mechanical stress due to airflow on these portions of the plant). Similarly, seed deposition was consistently predicted to be greatest in the middle of the plants' windward aspects. However, recirculation patterns differed considerably between the two cushion forms, with the periodic formation of eddies along both sides of the hemispherical plants (i.e. shedding of horseshoe vortices), and a more pronounced single vortex loop being shed behind the crescent cushions.

From a computational fluid dynamics perspective, airflow over a hemisphere or crescent on flat ground is challenging, since it necessitates the analysis of flow over two different surfaces (a flat plane and a curved surface) each with a unique surface roughness. Nonetheless, our results are in agreement with studies of flow around similar (but less complex) shapes. For example, in turbulent flow the separation point on a sphere has been reported to occur at 120° (Bakić, 2004; Bakić and Perić, 2005; Constantinescu and Squires, 2004), which closely matches our results. Similarly, both forms of flow recirculation and vortex shedding are well documented (Bakić, 2004; Bakić and Perić, 2005; Constantinescu and Squires, 2004). Additionally, from a biological perspective, the windward deposition of seeds against cushion plants predicted by the CFD model also matches field observations [e.g. (Bullock and Moy, 2004), although see (Aguiar and Sala, 1994)]. In this study variability in airflow speed (i.e.

gusting) was not considered, but it is known that changes in airflow velocity can affect the presence of a turbulent wake with recirculation (and the extent of the wake) (Bakić and Perić, 2005). Similarly, an increase in the turbulence intensity in the free stream airflow causes the position of the separation point to move further downstream (i.e. later separation of the boundary layer), decreases the recirculation zone, and increases mixing processes and particle entrainment (Bakić, 2004). As a result, under gusting conditions the extent of the recirculation zone behind cushion plants is likely to be more variable and, on average, probably smaller.

4. Conceptual model

Based on our results and on published data about *A. selago*, *A. magellanica* and sediment accumulation patterns, we propose a conceptual model for the development of crescent-shaped cushion plants. Our model makes two assumptions about differences in the growth of *A. selago* stems and the survival of *A. magellanica* grasses in exposed and sheltered conditions. First, we assume that direct wind damage through cooling, drying and scouring is minimal to intact cushion plants [although this is not true once a plant has started to lose its surface integrity; e.g. (Copson, 1984). This is a reasonable assumption given that the species' compact morphology reduces heat and water loss (e.g. xerophytic leaves) and minimizes physical damage to the leaves (Huntley, 1971; Schenck, 1905; Ternetz, 1902). Field observations support this assumption since there is a similar proportion of dead stems (and gaps due to the loss of stems) on the windward and leeward sides of hemispherical cushions [although see also (le Roux et al., 2005; Whinam et al., 2014).

Second, the model assumes that *A. magellanica* seedlings suffer higher mortality when exposed to strong winds than when they grow in more sheltered microsites. Indeed, the fine-scale distribution of mature *A. magellanica* on *A. selago* supports this assumption, with much higher cover of larger individuals of the grass on the cushion's leeward side (see also (Ashton and Gill, 1965; le Roux et al., 2005)), despite *A. magellanica* seedlings occurring on all aspects of cushion plants (PCLR, pers. obs.). This suggests that despite potentially far greater seed deposition on the exposed portions of the cushion plant and the ability for *A. magellanica* seeds to germinate on any part of a cushion, grasses are much more likely to survive in the lee of the hemispherical cushion where airflow velocity is much lower than the windward side. The distribution of the grass across topographic gradients also supports this assumption, with *A. magellanica* exhibiting higher densities in more wind-sheltered positions than in wind-exposed locations ((le Roux and McGeoch, 2010), see also (Pammenter et al., 1986)).

We summarize the process of crescent-shape cushion development into three stages, considering the deposition of seeds (irregularly shaped, with low mass and density) and sediment (smoother and denser than seeds, always being entrained from the soil surface) as two separate processes (Figure 31):

- 1) *Negligible air recirculation.* Airflow around a small, hemispherical cushion plant is relatively slow (due to the plant's low height) and there is little flow recirculation in its lee (and therefore negligible deposition of sediment). *A. magellanica* seeds are mainly deposited on the windward side of the cushion. While these seeds may germinate, they are unable to establish on the windward aspect of the cushion due to the strong scouring, cooling and drying effects of the direct wind.
- 2) *Sediment deposition and grass establishment.* As the cushion grows taller, airflow recirculation intensifies, leading to sediment deposition on the lee of the cushion. With stronger recirculation some *A. magellanica* seeds are also deposited on the lee of the cushion plant (although the majority are still deposited on the windward side of the plant) (see also (Aguiar and Sala, 1994)). The seeds deposited on the cushion's leeward aspect are more likely to establish due to the lower air velocities on that side of the plant. Additionally, the fine sediment that has accumulated in the lee of the plant may enhance seed trapping and survival (Chambers et al., 1991). As a result, *A. magellanica* biomass increases on the lee of the cushion. This causes the development of a positive feedback loop, with greater grass volume slowing airflow in the lee of the cushion even further, leading to increased deposition of sediment and seeds [(Pye and Tsoar, 1990; Ravi et al., 2008), see also (Cooke and Warren, 1973)].
- 3) *Differential cushion growth.* Due to shading (from grass growth) and burial (from sediment deposition; which also reduces incoming light) the cushion stems on the leeward side suffer disproportionately higher mortality [see also (Ashton and Gill, 1965; Hauri and Schröter, 1914) for other cushion plant species, (le Roux et al., 2005; Schöb et al., 2014)]. However, stem growth on the other sides of the cushion is unaffected, and as a consequence, the cushion develops a crescent shape. The change to the plant's shape in turn affects the plants aerodynamic characteristics, further enhancing air recirculation, leading to greater sediment and seed accumulation in the lee of the cushion. The intensification of recirculation on the sheltered side of the cushion plant also increases the wind protection for *A. magellanica*, favouring its continued growth and maintaining the positive feedback to crescent-shape development.

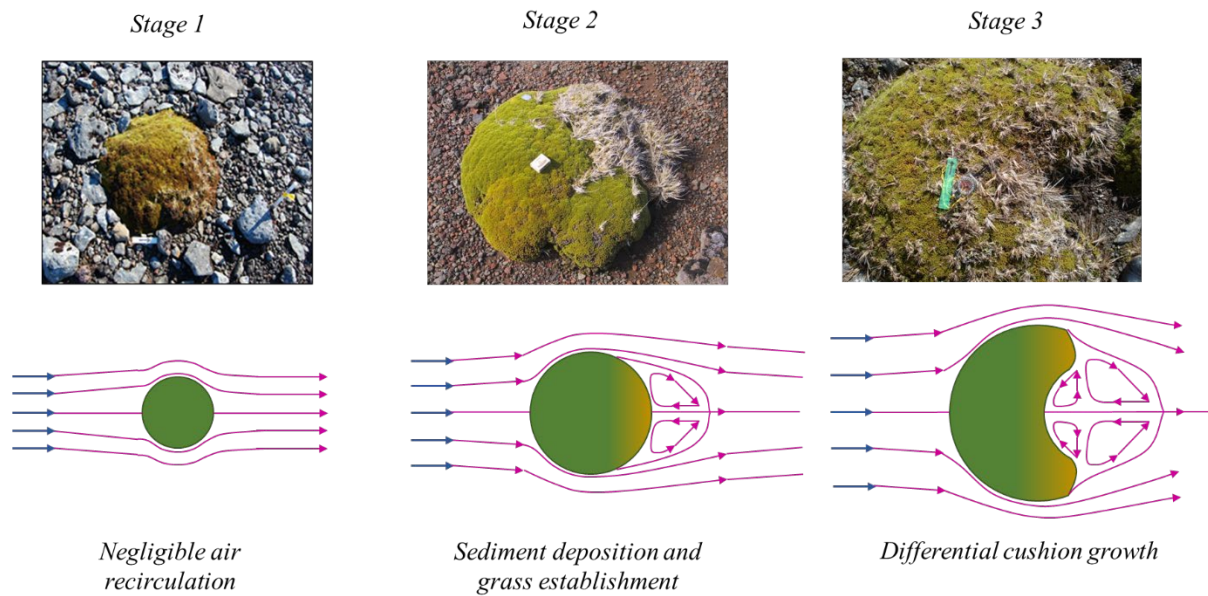


Figure 31: Graphical representation of the conceptual model for differential cushion growth

In areas lacking *A. magellanica* (or other epiphytes) the same stages of cushion shape development are likely to occur, because sediment deposition alone can still cause differential stem mortality on the wind- and leeward sides of *A. selago* cushions. Similarly, in the absence of wind-borne sediments, greater *A. magellanica* growth on the leeward sides of cushion plants may also be likely to be sufficient by itself to cause the development of crescent-shaped cushions. However, in the absence of either *A. magellanica* or sufficient wind-blown soil, the development of the crescent-shape is less likely to occur because there will be no positive feedback between grass growth and sediment trapping. As a result, our model may be applicable to the development of cushion plant shape in many windy environments, provided that adequate wind-borne sediment or seeds are present.

Our conceptual model is most appropriately applied to areas with sparse populations of *A. selago* with minimal other features that can act as wind disturbances (e.g. grey lava regions where the substrate is relatively flat). In black lava regions the substrate is more uneven and the ruggedness of the lava itself shapes the cushions (i.e. cushion plants, especially smaller individuals, grow between and around the taller shards of lava). Additionally, in dense or aggregated *A. selago* populations there may also be downstream wind flow impacts on cushion plants from upstream individuals too. However, *A. selago* plants generally do not have aggregate distributions locally [particularly for plants with diameters < 15 cm; (Nyakatya, 2006)], and there is typically a relatively even spacing between cushions (this likely reflects that the species root system extends far beyond individual cushion's canopies (Frenot et al., 1998)). Therefore, while there is potential for upstream plants to affect the wind flow

experienced by downstream plants, where the plants are uniformly or randomly spaced, there is some distance so that there will be some stabilization of flow between individuals. Nearest neighbour data for *A. selago* [e.g. (le Roux and McGeoch, 2004)] indicates that the distance to plants' nearest neighbours average 0.66 – 0.90 m (data from three different sites on Marion Island), and therefore, based on our CFD results (see e.g. Figure 9f which illustrates velocity profiles 0.4 m behind cushion plant), the wind conditions experienced by *A. selago* plants growing at typical densities will be minimally affected by upstream disturbances by other individuals.

Other mechanisms causing the development of crescent-shaped *A. selago* cushions have also been proposed. For example, it has been suggested that crescent-shaped cushions may develop due to leeward turf exfoliation by needle ice (Boelhouwers et al., 2003). This hypothesis posits that needle ice is disproportionately common in exposed soil on the leeward side of cushions (because air movement can inhibit needle ice formation), and therefore effects greater damage to the margin of the plant that is most sheltered from the wind. Upon damage to cushion stems (and the resultant loss of plant compactness) the organic soil underlying the plant is vulnerable to further needle ice formation and additional damage to stems. This hypothesis may be complementary with our model, because a greater proportion of fine sediments and enhanced moisture conditions (due to lower wind-driven evaporation) in the lee of the cushion is likely to favour needle-ice formation [(Pérez, 1987), see also e.g. (Holness, 2004)]. Indeed, the low plant cover observed in the exposed soil in the center of some crescent-shaped cushions may reflect regular needle-ice formation and active frost-heave processes [see e.g. (Boelhouwers et al., 2003)]. However, it seems unlikely that turf exfoliation alone would be able to initiate the leeward degradation of *A. selago* cushions [following e.g. (Butler et al., 2004; Pérez, 1992)], given the compact nature of the cushions and their buffering impact on cushion and soil temperatures (Arroyo et al., 2003; Chown and Crafford, 1992; Nyakatia and McGeoch, 2007). Additionally, needle ice is very rarely observed on intact cushion plants (Cavieres et al., 2007; Pérez, 1987). In coastal areas, greater deposition of salt-spray on the windward side of cushion plants could also drive the development of the crescent shape, as suggested by (Huntley, 1971), although salt-deposition alone seems unlikely to drive asymmetrical growth or stem mortality given the abundance of *A. selago* in the coastal areas of Marion Island (Gremmen, 1981). Therefore, while other mechanisms could also play a role in the development of crescent-shaped *A. selago* cushions, we suggest that wind-driven sediment and seed deposition initiates the change in plant shape. These mechanisms could also be the cause of other patterns of directionality observed in *A. selago* on Marion Island. For

example, because *A. magellanica* cover is highest on the sheltered leeward side of the cushion plants, it may indirectly drive higher densities of arthropods on the sheltered sides of *A. selago* cushions [the grass is thought to provide an extra food resource to the arthropods; (Hugo et al., 2004)].

5. Discussion

Our “leeward-deposition” model of cushion plant shape development generates some testable predictions. For example, on substrates with more turbulent airflow there should be less sediment accumulation on the leeward side of cushion plants. This results from a negative relationship between flow turbulence and the extent of recirculation in the lee of a sphere (Bakić, 2004). In consequence, a testable prediction from our model is that cushions will have less pronounced crescent shapes in habitats where airflow is more turbulent. Considering, for example, Marion Island, we would therefore predict less pronounced development of crescent-shapes in plants in fellfield areas with higher surface roughness (e.g. boulders and ridges or, more generally, post-glacial lava flows; increasing turbulence in the airflow) than in areas of lower surface roughness (i.e. relatively smooth soil surface; pre-glacial lava flows where glacial scouring has smoothed the landscape). Similarly, because substrates differ in their probability of entrainment by airflow (based on differences in particle density and size), sediment accumulation rates behind cushions are likely to vary between substrate types. As a result, our model predicts more pronounced crescent shapes for cushions growing in areas with small particles of low density (e.g. ash fields) than on substrates composed of larger, denser particles (e.g. scoria) provided the airflow is not too turbulent (i.e. subject to first prediction).

At the scale of individual plants, the model predicts that the mortality of leeward stems will expose humus that had developed in that portion of the cushion plant. Therefore, we expect the soil in the hollow of crescent-shaped cushions to have higher organic matter content than the surrounding mineral soils (at least in the upper surface layers). Furthermore, the sizes of sediment particles present in the hollow of crescent-shaped cushions should represent a subset of the available particles present in the surrounding soil, with an over-representation of particles that are light enough to be entrained by the prevailing winds. This prediction provides a strong test to distinguish between our model and the leeward turf exfoliation model (Boelhouwers et al., 2003), because needle ice-driven turf exfoliation is likely to favour the movement of fine particles away from the crescent by loosening the soil surface [although this may only be pronounced during times of soil dryness; (Pérez, 1992), leaving a heavier subset of particles present in the surrounding soil. Finally, the model also predicts that if cushions that

are exposed to the prevailing wind are subsequently experimentally sheltered, the *A. magellanica* seeds which were deposited on the windward side of the cushion will have higher establishment success. Furthermore, after wind sheltering is imposed, crescent-shape development is expected to slow considerably relative to plants still exposed to the prevailing wind [although to verify this would require long-term monitoring due to the slow growth of *A. selago*; (le Roux and McGeoch, 2004).

6. Conclusion

Cushion plants are an important vegetation component of many windy environments (Aubert et al., 2014). Due their slow growth rates and constrained growth forms, cushion plants may be sensitive to the direct (e.g. changes in temperature) and indirect (e.g. altered biotic interactions) effects of climate change [e.g. (le Roux et al., 2005)]. Our results suggest that cushion plants may also be sensitive to changes in wind patterns [see, e.g., (Bergstrom et al., 2015)]. While weakening winds are likely to favour the growth of competitors, rapid changes in wind conditions, as have occurred in the past at high latitudes in the southern hemisphere (Buizert et al., 2018), could affect cushion survival. If the prevailing wind direction changes after a cushion has developed directionality (i.e. its crescent-shape), cushions will experience increased stem mortality in different areas (because different portions of the plants will now comprise its wind- and leeward sides). For example, on Marion Island the decrease in wind speed variability over the last half century (le Roux and McGeoch, 2008) may have strengthened the development of the crescent-shape in *A. selago* cushions. By contrast, the shift in mean wind direction on the island (Rouault et al., 2005) could have caused a change in the directionality of young cushions. Indeed, if the directionality of cushion plant growth is relatively stable after the development of the crescent shape, the directionality of different cohorts of crescent-shaped cushions may be a guide to past wind patterns.

Acknowledgements

The South African National Research Foundation (NRF) and the South African National Antarctic Program (SANAP; unique grant number 110726) are thanked for their financial and logistic support. PCLR was additionally supported by the DST-NRF Center of Excellence for Invasion Biology. We thank C. Hui, J. Lee and E. Phiri for thoughtful comment on earlier drafts of this manuscript.

References

- Achenbach, E., 1974. Vortex shedding from spheres. *J. Fluid Mech.* 62, 209–221. <https://doi.org/DOI:10.1017/S0022112074000644>
- Achenbach, E., 1972. Experiments on the flow past spheres at very high Reynolds numbers. *J. Fluid Mech.* 54, 565–575. <https://doi.org/DOI:10.1017/S0022112072000874>
- Aguiar, M.R., Sala, O.E., 1994. Competition, facilitation, seed distribution and the origin of patches in a Patagonian steppe. *Oikos* 70, 26–34.
- Anderson Jr, J.D., 2015. *Introduction to Flight*, 8th ed. McGraw Hill, USA.
- Arroyo, M.T.K., Cavieres, L.A., Peñaloza, A., Arroyo-Kalin, M.A., 2003. Positive associations between the cushion plant *Azorella monantha* (Apiaceae) and alpine plant species in the Chilean Patagonian Andes. *Plant Ecol.* 169, 121–129. <https://doi.org/DOI:10.1023/A:1026281405115>
- Ashton, D.H., Gill, A.M., 1965. Pattern and process in a Macquarie Island feldmark. *Proc. R. Soc. Vic.* 79, 235–245.
- Aubert, S., Boucher, F., Lavergne, S., Renaud, J., Choler, P., 2014. 1914–2014: A revised worldwide catalogue of cushion plants 100 years after Hauri and Schröter. *Alp. Bot.* 124, 59–70. <https://doi.org/DOI:10.1007/s00035-014-0127-x>
- Badano, E., Marquet, P., 2008. Ecosystem engineering affects ecosystem functioning in high-Andean landscapes. *Oecologia* 155, 821–829. <https://doi.org/DOI:10.1007/s00442-007-0953-2>
- Badano, E.I., Cavieres, L.A., 2006. Impacts of ecosystem engineers on community attributes: effects of cushion plants at different elevations of the Chilean Andes. *Divers. Distrib.* 12, 388–396. <https://doi.org/DOI:10.1111/j.1366-9516.2006.00248.x>
- Badano, E.I., Villarroel, E., Bustamante, R.O., Marquet, P.A., Cavieres, L.A., 2007. Ecosystem engineering facilitates invasions by exotic plants in high-Andean ecosystems. *J. Ecol.* 95, 682–688. <https://doi.org/DOI:10.1111/j.1365-2745.2007.01262.x>
- Bakić, V., 2004. Experimental investigation of a flow around a sphere. *Therm. Sci.* 8, 63–81.
- Bakić, V., Perić, M., 2005. Visualization of flow around sphere for Reynolds number between 22 000 and 400 000. *Thermophys. Aeromechanics* 12, 307–314.
- Baumeister, D., Callaway, R.M., 2006. Facilitation by *Pinus flexilis* during succession: A hierarchy of mechanisms benefits other plant species. *Ecology* 87, 1816–1830. [https://doi.org/DOI:10.1890/0012-9658\(2006\)87\[1816:FBPFDS\]2.0.CO;2](https://doi.org/DOI:10.1890/0012-9658(2006)87[1816:FBPFDS]2.0.CO;2)
- Berg, J., Mann, J., Bechmann, A., Courtney, M.S., Jørgensen, H.E., 2011. The Bolund Experiment, Part I: Flow Over a Steep, Three-Dimensional Hill. *Bound.-Layer Meteorol.* 141, 219–243. <https://doi.org/10.1007/s10546-011-9636-y>
- Bergstrom, D.M., Bricher, P.K., Raymond, B., Terauds, A., Doley, D., McGeoch, M.A., Whinam, J., Glen, M., Yuan, Z.Q., Kiefer, K., Shaw, J.D., Bramely-Alves, J., Rudman, T., Mohammed, C., Lucieer, A., Visoiu, M., van Vuuren, B.J., Ball, M.C., 2015. Rapid collapse of a sub-Antarctic alpine ecosystem: the role of climate and pathogens. *J. Appl. Ecol.* 52, 774–783. <https://doi.org/DOI:10.1111/1365-2664.12436>
- Beyers, M., Waechter, B., 2008. Modeling transient snowdrift development around complex three-dimensional structures. *J. Wind Eng. Ind. Aerodyn.* 96, 1603–1615. <https://doi.org/DOI:10.1016/j.jweia.2008.02.032>

- Boelhouwers, J., Holness, S., Sumner, P., 2003. The maritime sub-Antarctic: a distinct periglacial environment. *Geomorphology* 52, 39–55. [https://doi.org/DOI:10.1016/S0169-555X\(02\)00247-7](https://doi.org/DOI:10.1016/S0169-555X(02)00247-7)
- Breuer, M., 2000. A challenging test case for large eddy simulation: high Reynolds number circular cylinder flow. *Int. J. Heat Fluid Flow* 21, 648–654. [https://doi.org/DOI:10.1016/S0142-727X\(00\)00056-4](https://doi.org/DOI:10.1016/S0142-727X(00)00056-4)
- Breuer, M., 1998. Numerical and modeling influences on large eddy simulations for the flow past a circular cylinder. *Int. J. Heat Fluid Flow* 19, 512–521. [https://doi.org/DOI:10.1016/S0142-727X\(98\)10015-2](https://doi.org/DOI:10.1016/S0142-727X(98)10015-2)
- Buizert, C., Sigl, M., Severi, M., Markle, B.R., Wettstein, J.J., McConnell, J.R., Pedro, J.B., Sodemann, H., Goto-Azuma, K., Kawamura, K., Fujita, S., Motoyama, H., Hirabayashi, M., Uemura, R., Stenni, B., Parrenin, F., He, F., Fudge, T.J., Steig, E.J., 2018. Abrupt ice-age shifts in southern westerly winds and Antarctic climate forced from the north. *Nature* 563, 681–685. <https://doi.org/10.1038/s41586-018-0727-5>
- Bullock, J.A., Moy, I.L., 2004. Plants as seed traps: inter-specific interference with dispersal. *Acta Oecologica* 25, 35–41. <https://doi.org/DOI:10.1016/j.actao.2003.10.005>
- Butler, D.R., Malanson, G.P., Resler, L.M., 2004. Turf-banked terrace treads and risers, turf exfoliation and possible relationships with advancing treeline. *Catena* 58, 259–274. <https://doi.org/DOI:10.1016/j.catena.2004.05.003>
- Cao, Y., Tamura, T., 2020. Large-eddy simulation study of Reynolds number effects on the flow around a wall-mounted hemisphere in a boundary layer. *Phys. Fluids* 32, 025109.
- Cavieres, L.A., Badano, E.I., Sierra-Almeida, A., Molina-Montenegro, M.A., 2007. Microclimatic modifications of cushion plants and their consequences for seedling survival of native and non-native herbaceous species in the High Andes of Central Chile. *Arct. Antarct. Alp. Res.* 39, 229–236. [https://doi.org/DOI:10.1657/1523-0430\(2007\)39\[229:MMOCPA\]2.0.CO;2](https://doi.org/DOI:10.1657/1523-0430(2007)39[229:MMOCPA]2.0.CO;2)
- CD-Adapco Group, 2008. *StarCD Methodology Manual v4.06*. CD-Adapco Group (<http://www.cd-adapco.com/>), London, UK.
- Cerfonteyn, M.E., le Roux, P.C., Van Vuuren, B.J., Born, C., 2011. Cryptic spatial aggregation of the cushion plant *Azorella selago* (Apiaceae) revealed by a multilocus molecular approach suggests frequent intraspecific facilitation under sub-Antarctic conditions. *Am. J. Bot.* 98, 909–914. <https://doi.org/DOI:10.3732/ajb.1000460>
- Chambers, J.C., Macmahon, J.A., Haefner, J.H., 1991. Seed entrapment in alpine ecosystems - effects of soil particle-size and diaspore morphology. *Ecology* 72, 1668–1677.
- Chown, S.L., Crafford, J.E., 1992. Microhabitat temperatures at Marion Island (46°54' S 37°45' E). *South Afr. J. Antarct. Res.* 22, 51–58.
- Chown, S.L., Froneman, P.W., 2008. *The Prince Edward Islands: Land-Sea Interactions in a Changing Ecosystem*. African SunMedia, Stellenbosch.
- Clift, R., Gauvin, W.H., 1970. The motion of particles in turbulent gas streams. *Proc. Chemeca* 70 1, 14–28.
- Combrinck, M.L., 2009. A computational fluid dynamic analysis of airflow over a keystone plant species, *Azorella selago* on sub-Antarctic Marion Island (MScEng thesis). Stellenbosch University, Stellenbosch.
- Constantinescu, G., Squires, K., 2004. Numerical investigations of flow over a sphere in the subcritical and supercritical regimes. *Phys. Fluids* 16, 1449–1466. <https://doi.org/DOI:10.1063/1.1688325>
- Cooke, R.U., Warren, A., 1973. *Geomorphology in Deserts*. University of California Press, Berkeley.

- Copson, G.R., 1984. An annotated atlas of the vascular flora of Macquarie Island, ANARE Research Notes 18. Australian National Antarctic Research Expeditions, Kingston, Tasmania.
- C.T. Crowe, Elger, D.F., Roberson, J.A., 2001. Engineering Fluid Mechanics, 7th ed. Wiley and Sons.
- de Langre, E., 2008. Effects of Wind on Plants. *Annu. Rev. Fluid Mech.* 40, 141–168. <https://doi.org/10.1146/annurev.fluid.40.111406.102135>
- Dehbi, A., Martin, S., 2011. CFD simulation of particle deposition on an array of spheres using an Euler/Lagrange approach. *Nucl. Eng. Des.* 241, 3121–3129. <https://doi.org/10.1016/j.nucengdes.2011.05.031>
- Durán, O., Herrmann, H.J., 2006. Vegetation against dune mobility. *Phys. Rev. Lett.* 97, 188001(4). [https://doi.org/DOI: 10.1103/PhysRevLett.97.188001](https://doi.org/DOI:10.1103/PhysRevLett.97.188001)
- Ennos, A.R., 1997. Wind as an ecological factor. *Trends Ecol. Evol.* 12, 108–111. [https://doi.org/DOI: 10.1016/S0169-5347\(96\)10066-5](https://doi.org/DOI:10.1016/S0169-5347(96)10066-5)
- Fitzgerald, N.B., Kirkpatrick, J.B., 2017. Wind distortion in alpine and subantarctic plants is constant among life forms but does not necessarily reflect prevailing wind direction. *Arct. Antarct. Alp. Res.* 49, 521–535. [https://doi.org/DOI: 10.1657/aaar0016-054](https://doi.org/DOI:10.1657/aaar0016-054)
- Flemmer, R.L.C., Banks, C.L., 1986. On the drag coefficient of a sphere. *Powder Technol.* 48, 217–221.
- Frenot, Y., Gloaguen, J.-C., Cannavacciuolo, M., Bellido, A., 1998. Primary succession on glacier forelands in the sub-Antarctic Kerguelen Islands. *J. Veg. Sci.* 9, 75–84.
- Frenot, Y., Gloaguen, J.-C., Picot, G., Bougère, J., Benjamin, D., 1993. *Azorella selago* Hook. used to estimate glacier fluctuations and climatic history in the Kerguelen Islands over the last two centuries. *Oecologia* 95, 140–144. [https://doi.org/DOI: 10.1007/BF00649517](https://doi.org/DOI:10.1007/BF00649517)
- G. M. Courtin, L. C. Bliss, 1971. A hydrostatic lysimeter to measure evapotranspiration under remote field conditions. *Arct. Alp. Res.* 3, 81–89.
- Garratt, J., 1994. Review: the atmospheric boundary layer. *Earth-Sci. Rev.* 37, 89–134. [https://doi.org/10.1016/0012-8252\(94\)90026-4](https://doi.org/10.1016/0012-8252(94)90026-4)
- Gauslaa, Y., 1984. Heat resistance and energy budget in different Scandinavian plants. *Holarct. Ecol.* 7, 5–78. [https://doi.org/DOI: 10.1111/j.1600-0587.1984.tb01098.x](https://doi.org/DOI:10.1111/j.1600-0587.1984.tb01098.x)
- Grace, J., 1977. Plant response to wind. Academic Press, London.
- Greeley, R., Iversen, J.D., 1985. Wind as a geological process on Earth, Mars, Venus and Titan, Cambridge Planetary Science Series. Cambridge University Press, Cambridge.
- Greene, D.F., Quesada, M., 2005. Seed size, dispersal, and aerodynamic constraints within the Bombacaceae. *Am. J. Bot.* 92, 998–1005. [https://doi.org/DOI: 10.3732/ajb.92.6.998](https://doi.org/DOI:10.3732/ajb.92.6.998)
- Gremmen, N.J.M., 1981. The vegetation of the sub-Antarctic islands, Marion and Prince Edward. Junk, The Hague.
- H. Schlichting, 1968. Boundary-Layer Theory, 3rd ed. McGraw-Hill.
- Hager, J., Faggi, A.M., 1990. Observaciones sobre distribución y microclima de cojines enanos de la Isla de Creta y del noroeste de la Patagonia. *Parodiana* 6, 109–127.
- Hauri, H., 1912. *Anabasis aretioides* Moq. and Coss., eine Polsterpflanze der algerischen Sahara: Mit einem Anhang, die Kenntnis der angiospermen Polsterpflanzen überhaupt betreffend. *Beih. Zum Bot. Cent.* 28, 323–421.
- Hauri, H., Schröter, C., 1914. Versuch einer Übersicht der siphonogamen Polsterpflanzen. *Bot. Jahrb. Für Syst. Pflanzengesch. Pflanzengeogr.* 50 (Suppl.), 618–656.
- Hausmann, N.S., McGeoch, M.A., Boelhouwers, J.C., 2009. Interactions between a cushion plant (*Azorella selago*) and surface sediment transport on sub-Antarctic Marion Island. *Geomorphology*. <https://doi.org/DOI:10.1016/j.geomorph.2008.12.002>

- Hoffman, J., 2006. Simulation of Turbulent Flow Past Bluff Bodies on Coarse Meshes Using General Galerkin Methods: Drag Crisis and Turbulent Euler Solutions. *Comput. Mech.* 38, 390–402. <https://doi.org/10.1007/s00466-006-0053-x>
- Holness, S.D., 2004. Sediment movement rates and processes on cinder cones in the maritime Subantarctic (Marion Island). *Earth Surf. Process. Landf.* 29, 91–103. <https://doi.org/DOI: 10.1002/esp.1015>
- Houghton, E.L., Carpenter, P.W., 1993. *Aerodynamics for engineering students*, 4th edn. ed. Arnold, London.
- Hugo, E.A., McGeoch, M.A., Marshall, D.J., Chown, S.L., 2004. Fine scale variation in microarthropod communities inhabiting the keystone species *Azorella selago* on Marion Island. *Polar Biol.* 27, 466–473. <https://doi.org/DOI: 10.1007/s00300-004-0614-4>
- Huntley, B.J., 1972. Notes on the ecology of *Azorella selago* Hook. f. *J. South Afr. Bot.* 38, 103–113.
- Huntley, B.J., 1971. Vegetation, in: van Zinderen Bakker, E.M., Winterbottom, J.M., Dyer, R.A. (Eds.), *Marion and Prince Edward Islands: Report on the South African Biological and Geological Expeditions, 1965 - 1966*. A.A. Balkema, Cape Town, pp. 98–160.
- Huntley, B.J., 1970. Altitudinal distribution and phenology of Marion Island vascular plants. *Tydskr. Vir Natuurwetenskap* 10, 255–262.
- Kim, J.-J., Baik, J.-J., 2003. Effects of inflow turbulence intensity on flow and pollutant dispersion in an urban street canyon. *J. Wind Eng. Ind. Aerodyn.* 91, 309–329. [https://doi.org/DOI: 10.1016/S0167-6105\(02\)00395-1](https://doi.org/DOI: 10.1016/S0167-6105(02)00395-1)
- Körner, C., 2003. *Alpine plant life: functional plant ecology of high mountain ecosystems*, 2nd ed. ed. Springer-Verlag, Heidelberg.
- Kullman, L., 2005. Wind-conditioned 20th century decline of birch treeline vegetation in the Swedish Scandes. *Arctic* 58, 286–294.
- le Roux, P.C., 2008. *Climate change and vascular plant species interactions on sub-Antarctic Marion Island* (PhD thesis). Stellenbosch University, Stellenbosch.
- le Roux, P.C., McGeoch, M.A., 2010. Interaction intensity and importance along two stress gradients: adding shape to the stress-gradient hypothesis. *Oecologia* 162, 733–745. <https://doi.org/DOI:10.1007/s00442-009-1484-9>
- le Roux, P.C., McGeoch, M.A., 2008. Changes in climate extremes, variability and signature on sub-Antarctic Marion Island. *Clim. Change* 86, 309–329. <https://doi.org/DOI: 10.1007/s10584-007-9259-y>
- le Roux, P.C., McGeoch, M.A., 2004. The use of size as an estimator of age in the subantarctic cushion plant, *Azorella selago* (Apiaceae). *Arct. Antarct. Alp. Res.* 36, 509–517. [https://doi.org/DOI: 10.1657/1523-0430\(2004\)36\[509:TUOSAA\]2.0.CO;2](https://doi.org/DOI: 10.1657/1523-0430(2004)36[509:TUOSAA]2.0.CO;2)
- le Roux, P.C., McGeoch, M.A., Nyakatia, M.J., Chown, S.L., 2005. Effects of a short-term climate change experiment on a sub-Antarctic keystone plant species. *Glob. Change Biol.* 11, 1628–1639. <https://doi.org/DOI: 10.1111/j.1365-2486.2005.001022.x>
- Lynch, A.J.J., Kirkpatrick, J.B., 1995. Pattern and process in alpine vegetation and landforms at Hill One, Southern Range, Tasmania. *Aust. J. Bot.* 43, 537–554. <https://doi.org/DOI: 10.1071/BT9950537>
- Lyotard, N., Shew, W.L., Bocquet, L., Pinton, J.-F., 2007. Polymer and surface roughness effects on the drag crisis for falling spheres. *Eur. Phys. J. B* 60, 469–476. <https://doi.org/10.1140/epjb/e2008-00018-0>
- Meas, M.R., Bruwer, J.F., Harms, T.M., Combrinck, M.L., n.d. Simulating Turbulent Air Flow Past a Hemispherical Body. *RD J. South Afr. Inst. Mech. Eng.* 6.

- Norberg, C., 1987. Effects of Reynolds number and low-intensity free-stream turbulence on the flow around a circular cylinder. Publication number 87/2. Department of Applied Thermodynamics and Fluid Mechanics, Chalmers University of Technology, Gothenburg, Sweden.
- Nyakatya, M., McGeoch, M.A., 2007. The microclimate associated with a keystone plant species (*Azorella selago* Hook. (Apiaceae)) on Marion Island. *Polar Biol.* 31, 139–151.
- Nyakatya, M.J., 2006. Patterns of variability in *Azorella selago* Hook. (Apiaceae) on sub-Antarctic Marion Island: climate change implications. University of Stellenbosch.
- Pammenter, N.W., Drennan, P.M., Smith, V.R., 1986. Physiological and anatomical aspects of photosynthesis of two *Agrostis* species at a sub-Antarctic island. *New Phytol.* 102, 143–160. <https://doi.org/DOI: 10.1111/j.1469-8137.1986.tb00806.x>
- Pérez, F.L., 1992. Processes of turf exfoliation (Rasenabschalung) in the high Venezuelan Andes. *Z. Für Geomorphol.* 36, 81–106.
- Pérez, F.L., 1987. Needle-ice activity and the distribution of stem-rosette species in a Venezuelan páramo. *Arct. Alp. Res.* 19, 135–153.
- Perry, R.H., Chilton, C.H., 1973. *Chemical Engineers' Handbook*, 5th edn. ed. McGraw-Hill Kogakusha, Tokyo.
- Petersen, E.L., Mortensen, N.G., Landberg, L., Højstrup, J., Frank, H.P., 1998. Wind power meteorology. Part I: climate and turbulence. *Wind Energy* 1, 2–22. [https://doi.org/DOI: 10.1002/\(SICI\)1099-1824\(199809\)1:1<2::AID-WE15>3.0.CO;2-Y](https://doi.org/DOI: 10.1002/(SICI)1099-1824(199809)1:1<2::AID-WE15>3.0.CO;2-Y)
- Phiri, E.E., McGeoch, M.A., Chown, S.L., 2009. Spatial variation in structural damage to a keystone plant species in the sub-Antarctic: interactions between *Azorella selago* and invasive house mice. *Antarct. Sci.* 21, 189–196. <https://doi.org/DOI: 10.1017/S0954102008001569>
- Pye, K., Tsoar, H., 1990. *Aeolian sand and sand dunes*. Unwin Hyman, London.
- Pyšek, P., Liška, J., 1991. Colonization of *Sibbaldia tetrandra* cushions on alpine scree in the Pamiro-Alai Mountains, Central Asia. *Arct. Alp. Res.* 23, 263–272.
- Raithby, G.D., Eckert, E.R.G., 1968. The effect of support position and turbulence intensity on the flow near the surface of a sphere. *Wärme- Stoffübertrag.* 1, 87–94. <https://doi.org/DOI: 10.1007/BF00750790>
- Ralph, C.P., 1978. Observations on *Azorella compacta* (Umbelliferae), a tropical Andean cushion plant. *Biotropica* 10, 62–67.
- Rauh, W., 1939. Über polsterförmigen Wuchs, ein Beitrag zur Kenntnis der Wuchsformen der höheren Pflanzen. *Nova Acta Leopoldina* 7, 267–508.
- Ravi, S., D'Odorico, P., Wang, L., Collins, S., 2008. Form and function of grass ring patterns in arid grasslands: the role of abiotic controls. *Oecologia* 158, 545–555. <https://doi.org/DOI: 10.1007/s00442-008-1164-1>
- Rouault, M., Mélice, J.-L., Reason, C.J.C., Lutjeharms, J.R.E., 2005. Climate variability at Marion Island, Southern Ocean, since 1960. *J. Geophys. Res.-Oceans* 110, C05007.1-C05007.9. <https://doi.org/DOI: 10.1029/2004JC002492>
- Ruffier-Lanche, R., 1964. Les plantes en coussinet. *Bull. Société Amat. Jard. Alp.* 4, 3–13.
- Ruthsatz, B., 1978. Las plantas en cojín de los semi-desiertos andinos del Noroeste Argentino. *Darwiniana* 21, 491–539.
- Savory, E., Toy, N., 1985. The flow regime in the turbulent near wake of a hemisphere. *Exp. Fluids* 4, 181–188. <https://doi.org/DOI: 10.1007/BF00717812>
- Schenck, H., 1905. Vergleichende Darstellung der Pflanzengeographie des Subantarktischen Inseln : insbesondere über Flora und Vegetation von Kerguelen, in: Chun, C. (Ed.),

- Deutsche Tiefsee-Expedition 1898-1899, Band II, Teil I. Gustav Fischer, Jena, pp. 1–178.
- Schiller, L., Naumann, Z., 1933. A drag coefficient correlation. *Z. Vereines Dtsch. Ingenieure* 77, 318–320.
- Schöb, C., Michalet, R., Cavieres, L.A., Pugnaire, F.I., Brooker, R.W., Butterfield, B.J., Cook, B.J., Kikvidze, Z., Lortie, C.J., Xiao, S., Al Hayek, P., Anthelme, F., Cranston, B.H., García, M.-C., Le Bagousse-Pinguet, Y., Reid, A.M., le Roux, P.C., Lingua, E., Nyakatya, M.J., Touzard, B., Zhao, L., Callaway, R.M., 2014. A global analysis of bi-directional interactions in alpine plant communities shows facilitators experiencing strong reciprocal fitness costs. *New Phytol.* 202, 95–105.
- Schulze, B.R., 1971. The climate of Marion Island, in: van Zinderen Bakker, E.M., Winterbottom, J.M., Dyer, R.A. (Eds.), *Marion and Prince Edward Islands: Report on the South African Biological and Geological Expeditions, 1965 - 1966*. A.A. Balkema, Cape Town, pp. 16–31.
- Selkirk-Bell, J.M., Selkirk, P.M., 2013. Vegetation-banked terraces on Subantarctic Macquarie Island: a reappraisal. *Arct. Antarct. Alp. Res.* 45, 261–274. <https://doi.org/DOI: 10.1657/1938-4246-45.2.261>
- Smith, V.R., 2002. Climate change in the sub-Antarctic: an illustration from Marion Island. *Clim. Change* 52, 345–357. <https://doi.org/DOI: 10.1023/A:1013718617277>
- Smith, V.R., Steenkamp, M., Gremmen, N.J.M., 2001. Terrestrial habitats on sub-Antarctic Marion Island: their vegetation, edaphic attributes, distribution and response to climate change. *South Afr. J. Bot.* 67, 641–654.
- Spomer, G.G., 1964. Physiological ecology studies of alpine cushion plants. *Physiol. Plant.* 17, 717–724.
- Tavakol, M.M., Abouali, O., Yaghoubi, M., 2015. Large eddy simulation of turbulent flow around a wall mounted hemisphere. *Appl. Math. Model.* 39, 3596–3618. <https://doi.org/10.1016/j.apm.2014.11.055>
- Tavakol, M.M., Yaghoubi, M., Masoudi Motlagh, M., 2010. Air flow aerodynamic on a wall-mounted hemisphere for various turbulent boundary layers. *Exp. Therm. Fluid Sci.* 34, 538–553. <https://doi.org/10.1016/j.expthermflusci.2009.11.007>
- Taylor, B.W., 1955a. Terrace formation on Macquarie Island. *J. Ecol.* 43, 133–137.
- Taylor, B.W., 1955b. The flora, vegetation and soils of Macquarie Island, Australian national Antarctic research expeditions reports: series B, volume II. Antarctic division, Department of External Affairs, Melbourne.
- Ternetz, C., 1902. Morphologie und anatomie de *Azorella selago* Hook. f. *Bot. Ztg.* 60, 1–19.
- Tiwari, S.S., Pal, E., Bale, S., Minocha, N., Patwardhan, A.W., Nandakumar, K., Joshi, J.B., 2020. Flow past a single stationary sphere, 1. Experimental and numerical techniques. *Powder Technol.* 365, 115–148. <https://doi.org/10.1016/j.powtec.2019.01.037>
- van Gardingen, P.R., Grace, J., Jeffree, C.E., 1991. Abrasive damage by wind to the needle surfaces of *Picea sitchensis* (Bong.) Carr. and *Pinus sylvestris* L. *Plant Cell Environ.* 14, 185–193. <https://doi.org/10.1111/j.1365-3040.1991.tb01335.x>
- Versteeg, H., Malalasekera, W., 2007. *An Introduction to Computational Fluid Dynamics: The Finite Volume Method*, 2nd edition. ed. Pearson Prentice Hall, United Kingdom.
- Whinam, J., Abdul-Rahman, J.A., Visoiu, M., di Folco, M.B.F., Kirkpatrick, J.B., 2014. Spatial and temporal variation in damage and dieback in a threatened subantarctic cushion species. *Aust. J. Bot.* 62, 10–21. <https://doi.org/DOI: 10.1071/bt13207>
- White, F.M., 2016. *Fluid Mechanics*, 8th ed. McGraw Hill, USA.
- Whitehead, F.H., 1951. Ecology of the Altipiano of Monte Maiella, Italy. *J. Ecol.* 39, 330–355.

- Wilson, J.W., 1959. Notes on Wind and its Effects in Arctic-Alpine Vegetation. *J. Ecol.* 47, 415. <https://doi.org/10.2307/2257374>
- Yang, W., Quan, Y., Jin, X., Tamura, Y., Gu, M., 2008. Influences of equilibrium atmosphere boundary layer and turbulence parameter on wind loads of low-rise buildings. *J. Wind Eng. Ind. Aerodyn.* 96, 2080–2092. <https://doi.org/DOI: 10.1016/j.jweia.2008.02.014>
- Zhang, Q.H., Miao, T.D., 2003. Aeolian sand ripples around plants. *Phys. Rev. E* 67, 051304(4). <https://doi.org/DOI: 10.1103/PhysRevE.67.051304>
- Zotz, G., Schweikert, A., Jetz, W., Westerman, H., 2000. Water relations and carbon gain are closely related to cushion size in the moss *Grimmia pulvinata*. *New Phytol.* 148, 59–67. <https://doi.org/DOI: 10.1046/j.1469-8137.2000.00745.x>